JOURNAL OF PROPULSION AND POWER
Vol. 25, No. 1, January–February 2009

Microwave and Direct-Current Discharges in High-Speed Flow: Fundamentals and Application to Ignition

Valery M. Shibkov,* Andrei F. Aleksandrov,* Vladimir A. Chernikov,† Aleksei P. Ershov,† and Lidia V. Shibkova†
Moscow State University, 119992, Moscow, Russia

DOI: 10.2514/1.24803

The main parameters and properties of an electrodeless freely localized microwave discharge, a surface microwave discharge, transversal in relation to the gas flow direct-current and pulse-periodic electrode discharges, and a combined microwave direct-current discharge are experimentally investigated. It is shown that all types of the discharges result in a reliable ignition of hydrocarbon fuel. Combustion of a propane–air supersonic stream is realized under condition of the combined surface microwave and direct-current discharge. To find out the influence of different channels of energy transfer on ignition of combustible mixtures in a supersonic flow, the kinetic model of ignition of hydrocarbons–air mixtures, and taking into account the influence of electric field on processes of dissociation molecules and creation of the active radicals, excited and charged (electrons, positive and negative ions) particles under conditions of nonequilibrium plasma of the gas discharge was developed. Mathematical modeling has revealed a strong influence of the reduced electric field on induction period. The microwave discharges may find applications in different fields of supersonic plasma aerodynamics and in development of new-generation plasma sources for plasma chemistry, nano- and microelectronics purposes (plasma treatment of surfaces, etching, and film deposition), and so on.

Nomenclature

b_i	=	ion mobility
D_a	=	ambipolar diffusion coefficient
E/n	=	reduced electric field
L	=	discharge longitudinal length
M	=	flow Mach number
$n_{e,\mathrm{cr}}$	=	critical concentration of electrons
n_e	=	electron density
n	=	air density
p	=	air pressure
Q	=	period-to-pulse duration ratio
T_e	=	electron temperature
T_g	=	gas temperature
υ_d	=	discharge propagation velocity
υ_f	=	flow velocity
W_p	=	peak microwave power
λ	=	microwave wavelength
ν_a	=	attachment frequency
ν_D	=	diffusion frequency
ν_{en}	=	frequency of electron-neutral collisions
ν_i	=	ionization frequency
τ	=	pulse duration
ω	=	circular frequency of the electric field

I. Introduction

ADVANCES in aviation technology call for research and development aimed at creating new, efficient means for controlling the gas flow parameters near an aircraft's surface, heat and mass transfer in the boundary layer, and flow separation, reducing the frontal and surface friction, and delaying the laminar–turbulent transition, as well as for reducing the ignition time and controlling the combustion of supersonic fuel flow in a ramjet engine. A new solution to these problems is application of different gas discharges. This has given rise to a new field of research in plasma physics, supersonic plasma aerodynamics, which is rapidly progressing today [1,2]. Specifically, it is conjectured that placement of a plasma object in front of and on the lifting surfaces of the vehicle will improve its aerodynamic characteristics, and use of a nonequilibrium gas-discharge plasma will reduce the fuel ignition time in a hypersonic ramjet engine.

The mechanism of the gas-phase oxidation of various combustible gases, including hydrocarbons and hydrogen, has been thoroughly studied (see, e.g., [3–10]), with the emphasis on their ignition mechanism. The great majority of publications in this field have dealt with factors determining the induction period preceding the ignition event. In recent decades, there has also been much literature discussing the possibility of effectively controlling combustion processes by various physical means. For example, Semenov [11] studied the broadening of the inflammability range of the hydrogen–oxygen mixture under the action of shortwave radiation or oxygen atoms. Furthermore, it has been experimentally demonstrated that, under the action of ultraviolet radiation $\lambda = 175$ nm, the inflammability "peninsula" broadens and shifts to lower temperatures [12]. In a number of works, it is suggested to initiate ion–molecule and ion–atom reactions using low-temperature gas-discharge plasma [1,2]. In the same works, plasma jets and laser radiation are discussed as possible ignitors for supersonic hydrocarbon streams. Numerical analysis and experimental studies of the ignition of argon- or helium-diluted H_2–O_2, H_2–air, and CH_4–O_2 mixtures with a nanosecond high-voltage discharge at various temperatures, mixture compositions and pressures, and energies deposited in the discharge have revealed marked distinctions between the equilibrium and nonequilibrium excitations of the mixtures [13]. The effects of the initial concentration of free radicals (H and O atoms) and of the radiolysis rates of dihydrogen and dioxygen on the ignition limits of the stoichiometric hydrogen–oxygen mixture have been studied by numerical simulation [14]. The ignition temperature near the first limit appeared to be the most sensitive to the dihydrogen and dioxygen radiolysis rates. The ignition of various hydrocarbon-containing combustible mixtures by laser heating or laser-induced breakdown has been studied as a function of gas pressure and laser wavelength [15–17]. Although this laser treatment exerts a strong effect on the ignition of the mixture, it

Received 30 January 2007; revision received 17 July 2008; accepted for publication 17 July 2008.

*Professor, Physical Faculty.
†Associate Professor, Physical Faculty.

suffers from an essential drawback as applied to hypersonic ramjets: it is impossible to initiate ignition in a large volume. The ignition of a propane–air supersonic flow by microwave discharges has been studied as a function of gas pressure, pulse duration, microwave power, equivalent ratio, and so on (see, e.g., [18–27] and the literature cited therein).

A cursory survey of the literature has demonstrated that there are numerous ways of intensifying the chain combustion of hydrocarbons. However, the ignition kinetics are not completely understood, even for the rather simple model system of hydrogen–oxygen under low-temperature gas-discharge plasma conditions, which are established at large values of the reduced electric field. Therefore, for a deeper insight in the physicochemical processes occurring in the low-temperature plasma initiation of the ignition of a combustible gas, the experimental study of the effect of a gas discharge on the ignition event should be accompanied by mathematical modeling. The study of the ignition and combustion of hydrogen-containing mixtures under low-temperature plasma conditions is of importance from various standpoints: it is necessary to carry out both fundamental research in the mechanism and kinetics of atom–molecule reactions in a strong electric field and an analysis of a variety of applied problems, including the optimization of plasma chemical processes. One practical problem is to develop the physical principles of the hypersonic ramjet. To diminish the ramjet length, it is necessary to ensure a rapid space ignition of the high-velocity hydrocarbon flow. To do this, it is necessary to minimize the induction period. It is known that ignition of combustible gaseous mixtures can be realized or due to heating of gas to a high temperature (thermal autoignition) or because of radicals and active particles. One of the principal goals of the investigations is to find out the mechanisms responsible for ignition at the presence of non-equilibrium low-temperature plasma of the gas discharge at high values of the reduced electric field.

The results of researches of low-temperature nonequilibrium microwave plasmas in still air and in supersonic streams of the air and hydrocarbon–air fuel which have been fulfilled at Physical Faculty of the Moscow State University [1,2,19–47] within last several years are submitted in this paper.

II. Experimental Installation

One of the aims of this paper is to study the main properties of a freely localized discharge produced by a focused microwave beam, as well as microwave discharge, forming on the external surface of a dielectric body by surface wave.

Most gas discharges are produced with the use of single- or multielectrode energy supply systems. From the practical standpoint, such systems are poorly suited to remotely control plasma production in a certain spatial region, for example, ahead of a body moving with a supersonic velocity in the atmosphere (rather than at its surface). Electrodeless systems in which freely localized discharges are produced using focused microwave beams are best suited for this purpose. In a freely localized discharge, the electric field is localized in the waist region of a focused microwave beam. Microwave beams can be focused in both still gases and gas flows. Gas breakdown in a microwave discharge occurs over a time that is shorter than the time during which the gas propagates through the discharge; therefore, the discharge is not blown off by the supersonic flow. A freely localized (electrodeless) microwave discharge is produced in a given spatial region by a focused high-power microwave beam. It is well known (see, e.g., [19–55] and the literature cited therein) that, if the electric field strength in the focal region of a focused microwave radiation exceeds a certain threshold value, gas breakdown occurs there. The plasma produced begins to efficiently absorb microwave energy. This leads to the efficient ionization, dissociation, and excitation of the gas in this region. The absorbed energy is redistributed among different components and degrees of freedom of the molecular gas.

The second type of microwave discharge is a surface microwave discharge. It is known [56–61] that, when a microwave discharge is initiated inside a gas-filled dielectric-wall tube, the electromagnetic energy applied to the system is converted into a surface wave. The resulting system is self-consistent: for the surface wave to exist, the plasma medium produced by the wave itself is necessary. The wave propagates in space as long as its energy suffices to produce a plasma with an electron concentration no lower than critical concentration $n_{e,\mathrm{cr}} = m(\omega^2 + \nu_{\mathrm{en}}^2)/(4\pi e^2)$, where e is the electron charge, m is the electron mass, ω is the circular frequency of the field, and ν_{en} is the frequency of electron-neutral collisions. The surface wave does not penetrate into the region where the electron concentration is below $n_{e,\mathrm{cr}}$, so that the surface discharge is absent there. Here, we are dealing with a plasma-insulator-free space system: a gas-filled low-pressure discharge tube contains a plasma produced by a surface wave, and this plasma is separated from the environment by the dielectric walls. In our investigations, we turn the system considered here inside out: the plasma covers an insulator on the surface of which a plasma-sustaining microwave electromagnetic wave is generated. This type of microwave discharge initiated on insulators by a surface wave has been considered in [44–48]. The plasma region may be made extended and variously shaped in a wide range of electromagnetic radiation energies and frequencies.

Experiments were carried out on the installation, consisting of a vacuum chamber, a receiver of a high pressure of air, a receiver of a high pressure of propane, a system for mixing propane with air, a system for producing a supersonic gas flow, two magnetron generators, two systems for delivering microwave power to the chamber, cylindrical and rectangular aerodynamic channels, two sources of high-voltage pulses, a synchronization unit, and a diagnostic system (see Fig. 1). The basic component of the experimental setup is an evacuated metal cylindrical chamber, which serves simultaneously for supersonic flow creation and as a tank for the expiration of gases or combustion products. The inner diameter of the vacuum chamber is 1 m and its length is 3 m. A supersonic flow was produced by filling the vacuum chamber with air through a specially profiled Laval nozzle mounted on the outlet tube of the electromechanical valve. In our experiments, we used cylindrical and rectangular nozzles designed for a Mach number of $M = 2$.

The microwave source is a pulsed magnetron generator operating in the centimeter wavelength range. The parameters of the magnetron generator are as follows: the wavelength is $\lambda = 2.4$ cm, the pulsed microwave power is $W_p < 200$ kW, the pulse duration is $\tau = 1$–200 μs, and the period-to-pulse duration ratio is $Q = 1000$. The magnetron is powered from a pulsed modulator with a partial discharge of the capacitive storage. Microwave power was delivered to the discharge chamber through a 9.5×19 mm rectangular waveguide. The input microwave power was measured with the help

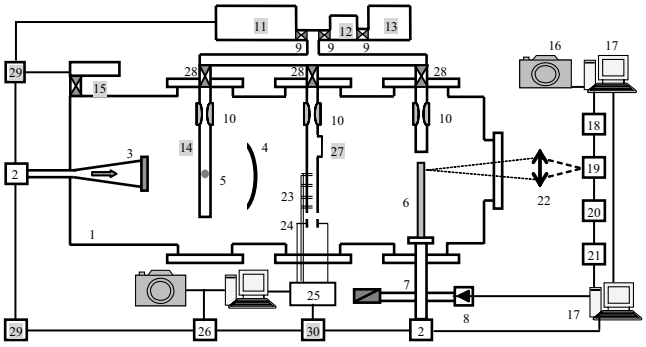

Fig. 1 Block diagram of the experimental setup: 1) vacuum chamber, 2) magnetrons, 3) horn antenna, 4) metal mirror, 5) freely localized microwave discharge, 6) surface microwave discharge, 7) waveguide with directional coupler, 8) crystal microwave detector, 9) valves, 10) Laval nozzles, 11) air high-pressure receiver, 12) propane high-pressure receiver, 13) high-pressure cylinder with propane, 14) cylindrical aerodynamic channel, 15) pump out, 16) video and photo camera, 17) computers, 18) digital oscilloscope, 19) monochromator, 20) CCD sensor or photomultiplier tube, 21) shadow graphics installation, 22) lens, 23) double probes, 24) plane capacitor, 25) data gathering system, 26) control systems, 27) rectangular aerodynamic channel with cavity, 28) electric hydraulic valves, 29) synchronization units, 30) power supply systems.

of a directional coupler installed in the waveguide, so that a fraction of microwave power was directed to the measuring arm containing an attenuator and a section with a crystal detector. All the components of the microwave transmission line were sealed. To avoid electric breakdowns inside the waveguide, it was filled with an insulating gas (SF_6) at a pressure of 4 atm. The vacuum system of the chamber allows us to vary the pressure over a wide range, from 10^{-3} to 10^3 torr.

We used two schemes for a freely localized microwave discharge exciting. In the first scheme, the microwave beam was focused by a 0.6-m-diam dielectric lens with a focal length of 0.8 m. However, to ignite fuels, we used another scheme for microwave discharges exciting (Fig. 1). In this scheme, a horn antenna and a metal short-focus mirror are used instead of the lens. The horn forms a microwave beam incident onto a spherical mirror. This mirror is positioned in front the horn. A microwave discharge in a supersonic flow is produced in a quartz smooth 3-cm-diam cylindrical aerodynamic channel without a stagnation zone located between the horn and the mirror, in the focal plane of the mirror. The supersonic flow was perpendicular to the propagation direction of the microwave beam.

For creation of a surface microwave discharge, a specially designed device was used to couple the waveguide end inserted into the discharge chamber to a dielectric (quartz or Teflon) antenna, on which a surface microwave discharge was initiated. We assume that the positive direction of the OX axis is aligned with the direction of microwave surface wave propagation along the antenna. The origin $x = 0$ is at the end of the waveguide, through which the electromagnetic energy initiating the surface discharge is applied to the antenna. The supersonic flow has been directed opposite to the direction of the discharge propagation.

The high-pressure air-supply system consists of a gas holder, with the high-pressure air compressor raising pressure up to maximum value of $p = 12$ atm, the high-pressure gauge, transducer of dynamic pressure, stop valve, and electromagnetic valve with an opening time of $t \sim 1$ ms. The system of storage and fuel supply consists of a standard reservoir, which contains a liquid propane. Through a stop valve and the reduction gearbox, a gas fuel already goes into a receiver. Air or an air–propane mixture originally goes into the mixing device, established in a subsonic part of a channel. Directly behind the mixer, the supersonic nozzle is arranged.

The aerodynamic channel of a rectangular section with a stagnation zone in the form of a rectangular cavity in a broad wall was used for investigation of the possibility of ignition of a supersonic propane–air mixture with the help of a transversal surface pulse-periodical electrode discharge. The discharge was formed on a dielectric flat plane placed on the bottom of a cavity. The high-voltage pulses led to electrodes built-in flush to a dielectric plate. It was possible to adjust the cavity depth, displacing a plate in a direction perpendicular to supersonic flow. Two power supplies were used. The first source gave a voltage $U = 10$–30 kV, pulse duration $\tau = 50$–1000 μs, thus discharge current $i = 5$–20 A. The second source gave a voltage $U = 2.5$–4.5 kV, duration of a pulse could change from 0.1 up to 2.0 s, and discharge current changed from 1 to 30 A.

The combined discharge is offered with the purpose of reduction of an induction period and increase of an intensification of combustion of a high-speed stream of hydrocarbon fuel. The discharge represents a combination of the pulse-periodic self-sustained surface microwave discharge and the direct-current discharge created in a recirculation zone of the aerodynamic channel. Thus, surface microwave discharge serves for the several purposes. First, it facilitates initiation of the direct-current discharge. Second, effective energy contribution to plasma takes place under conditions of the microwave discharge. It leads to effective creation of the active radicals, excited and charged particles, and also to intensive volumetric illumination of gas flow by ultraviolet radiation. The direct-current discharge serves for the contribution of a thermal energy to gas and stabilization of combustion of a hydrocarbon fuel stream. We used various types of stagnant zones: a reverse step, a rectangular cavity with various depths of forward and back walls, a rectangular cavity with angled rear wall, and a rectangular cavity. Pressure gauges made it possible to measure distribution of pressure in various points of the aerodynamic channel and to register ignition of a propane–airstream on change of pressure in the channel.

III. Diagnostic Techniques

In experiments, we used the following diagnostic equipment: 1) a set of spectroscopic equipment with digital registration of plasma spectra, 2) a set of electric probe equipment with digital registration of voltage-current characteristics, 3) a high-speed camera for registration of discharge dynamics, 4) installation of shadow diagnostics for registration of flame dynamics, 5) a digital photo camera and digital video camera, and 6) a system for measurement of conductivity of a flame and so on.

The translational gas temperature in a microwave discharge was determined by a spectroscopic method based on measuring the distribution of the line intensities in the rotational structure of the (0;2) band of the second positive system of molecular nitrogen ($\lambda = 380.5$ nm). The vibrational temperature was determined from the relative intensities of the bands of the second positive system of molecular nitrogen and molecular bands of cyanogen. When determining the translational and vibrational gas temperatures, the emission spectra from a microwave discharge were recorded with the help of spectrograph (with an inverse dispersion of 0.3–1.0 nm/mm) and two monochromators (with inverse dispersions of 0.3 and 1.0 nm/mm, respectively). As a detector, we used either a photomultiplier or a charge-coupled device (CCD) array (a photodiode unit consisting of a large number of light-sensitive elements arranged in line) positioned behind the exit slit of the monochromator. In our experiments, we used a CCD array consisting of 3650 elements, each 8×8 μm in size; this ensured spatial resolution of no worse than 0.4 mm. The data on electron concentration were obtained with help of the probe method and by the Stark broadening of the H_β ($\lambda = 486.1$ nm) line of hydrogen. The general view of a microwave discharge was photographed in two projections (side view and top view). Also, the discharge was recorded by a video camera. To measure the threshold characteristics of the surface microwave discharge, we recorded the minimal applied power at which the discharge is initiated on the antenna surface versus air pressure p in the chamber at various pulse durations τ.

The ignition of the supersonic stream was detected as a glow in the aerodynamic channel downstream of the discharge section. No glow was observed when a gas discharge was generated in an airflow, when it was generated in a supersonic propane-airflow, but its parameters (pulse duration, discharge current, electric field strength in the plasma, and the electric power deposited into discharge) were inappropriate for ignition, or when the mixture was far from stoichiometric. Induction time was simultaneously derived from different measurements: 1) the minimum microwave pulse duration resulting in a glowing flame in the aerodynamic channel downstream of the discharge section, 2) the time taken by the intensity of the molecular band of the excited CH^* radical [the (0;0) band of the $A^2\Delta \rightarrow X^2\pi$ transition], with a wavelength of $\lambda = 431.5$ nm, to achieve the maximum growth rate, 3) the time taken by the signal from the double probe to achieve the maximum growth rate, and 4) the time taken by the current through the plane capacitor at the outlet of the aerodynamic channel to achieve the maximum growth rate. The ignition of the supersonic flow was also detected as an increasing output signal from an acoustic noise meter, as a sharp change of general view of plasma radiation spectrum and as a sharp increase of gas temperature.

IV. Experimental Results

A. Freely Localized Microwave Discharge

The magnetron parameters allowed us to produce electrodeless discharges in a focused microwave beam at air pressures below 100 torr. At pressures higher than 100 torr, it was necessary to initiate the discharge externally because, in undercritical electric fields, the discharge cannot develop without a preliminary breakdown. The

discharge can be initiated, for example, by an intense laser pulse or by introducing an initiator (a metal needle or a special target) in the focal region of the microwave beam or by a spark discharge. At low pressures, the freely localized microwave discharge resembles a chain of plasmoids separated by a distance of about 1 cm. The transverse size of the plasmoids is one to several centimeters. At the threshold input power, the total length of the discharge decreases with increasing pressure. At high pressures (by high pressures, we mean pressures at which the inequality $\nu_{\text{eff}} \gg \omega$ holds, where ν_{eff} is the effective electron–molecule collision frequency and ω is the microwave circular frequency), the microwave discharge is highly nonuniform and consists of several bright plasma channels which are less that 1 mm in diameter and are extended along the microwave electric field.

Figure 2 shows the translational and vibrational gas temperatures as functions of the air pressure for the threshold incident power. It can be seen that the gas temperature increases monotonically from 500 to 1800 K as the air pressure increases from 10 to 100 torr. The increase in the temperature can be explained as follows: At the threshold microwave power, the breakdown field increases in proportion to the air density n. In this case, as the pressure increases, the reduced electric field E/n remains constant, whereas the electron density increases [32]. This leads to an increase in the energy deposited in the gas and, accordingly, to an increase in the gas temperature. At the same time, the vibrational temperature varies nonmonotonically with pressure and passes through a minimum at $p \sim 30$ torr. This pressure corresponds to the minimum in the Paschen curve for the given microwave wavelength, that is, the power required for initiating a freely localized microwave discharge is minimum at this pressure [32].

Studies of the molecular gas heating under conditions of a freely localized microwave discharge in air have revealed that, when the electric field is switched on, the molecular gas is rapidly heated with the rate of $dT_g/dt \sim 10^8$ K/s and this heating rate decreases sharply after a period of 10–20 μs, due to the discharge motion toward the source of radiation and because of the electric field decrease due to the skin effect [32]. To find out the basic mechanism responsible for fast gas heating, the mathematical modeling of the investigated phenomenon was carried out. For numerical modeling, we used a nonstationary kinetic model [29–39]. This model relies upon the Boltzmann equation for the electron energy distribution function, a set of gas dynamic balance equations for the populations of the vibrational levels of the ground and electron-excited states of nitrogen and oxygen and for the concentrations of reactive and charged plasma particles, and a nonstationary heat conduction equation for the gas temperature. The model allows for various processes influencing gas heating, such as heat transfer to the translational degrees of freedom via elastic electron–molecule collisions, rotational–translational relaxation, vibrational–translational relaxation (VT relaxation), vibrational–vibrational exchange (VV process), and quenching of electron-excited molecular states (AV and AA relaxation).

As demonstrated by the numerical calculation results (see Fig. 3, curve 6), the gas heating rate due to the quenching of electron-excited

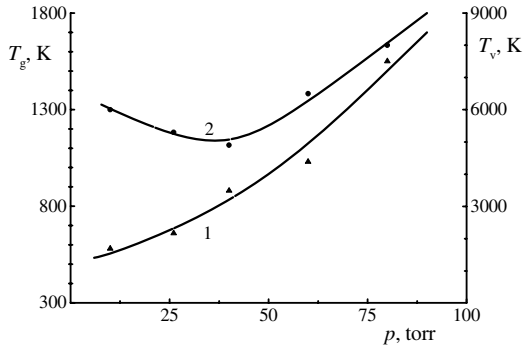

Fig. 2 Translational (1) and vibrational (2) gas temperature in the plasma of a freely localized microwave discharge as functions of the air pressure at the threshold microwave power.

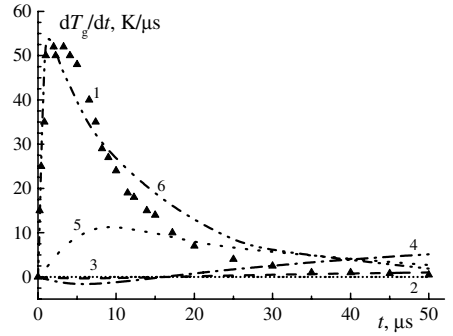

Fig. 3 Gas heating rate in the plasma of a freely localized microwave discharge in air vs time. Dots (1) indicate the experimental data, and curves the calculation results for (2) elastic interaction, (3) VT relaxation, (4) VV exchange, (5) AV relaxation, (6) AV and AA relaxation.

nitrogen molecules provides the observed gas heating rate. The experimental results were compared with the results of numerical calculation of the evolution of gas temperature in the active phase of a self-sustained microwave discharge and at the stage of afterglow. A satisfactory agreement between experiment and theory is observed. If the microwave field is switched off after a short time ($t = 5$ μs), which is too short for pumping energy to the low-lying vibrational levels, the gas as a whole cools down, due to the losses of energy into the surrounding space. If the microwave field is switched off after a long enough period ($t = 5$–10 μs), when the population of the low-lying vibrational levels of molecules is great, then, at the stage of plasma deionization, a further slow gas heating (with the rate of heating $\sim$0.1 K/μs) occurs due to the VV exchange and VT relaxation.

It was also shown that, at the initial stage of the microwave discharge in hydrogen, the gas heating rate exceeds 300 K/μs. It is much higher than in pure air plasma at microwave discharges at the same conditions. The estimations show that such a fast gas heating cannot be provided by either elastic heating, VT relaxation, or nonresonant VV exchange. In conditions of the experiment in hydrogen, the fast gas heating can be provided at the expense of the mechanism offered in [61]. This mechanism is connected with excitation unstable state $b^3\Sigma_u$ by electron impact in process: $H_2(X^1\Sigma_g) + e \rightarrow H_2(b^3\Sigma_u) + e \rightarrow H + H + e$. The state $b^3\Sigma_u$ breaks up to two hydrogen atoms for the time compared with a characteristic period of molecular fluctuations ($\sim 10^{-14}$ s). At this, a part of excitation energy of the state $b^3\Sigma_u$, equal to $E - E^D$ [where E^D is the dissociative energy limit of a term $H_2(b^3\Sigma_u)$], immediately transforms into the kinetic energy of gas.

The similar temporary evolution of gas temperature was experimentally observed by us during research of kinetics of gas heating in various types of the discharge in air, hydrogen, nitrogen, and a mixture of nitrogen with oxygen [29–42]. Experimental researches and theoretical calculation permit one to form a conclusion that, at large values of a reduced electric field $E/n > 100$ Td, the quenching of long-lived electronically excited states of molecules is one of main mechanisms responsible for fast heating of the molecular gases.

It is known [48–55] that the microwave discharges are inhomogeneous at gas pressures above 100–200 torr. The plasma formation consists of a large number of thin filaments (0.1–0.3 mm in diameter). The electron density in a channel of a microwave discharge in nitrogen was determined as a function of the gas pressure by the Stark broadening of the H_β ($\lambda = 4861$ Å) line of hydrogen. The electron density was deduced from the H_β profiles, taking into account broadening factors such as the instrumental function (about 0.01 nm), the Doppler effect (about 0.01 nm), the external microwave Stark effect (about 0.01 nm), and finite width of the monochromator slit. The electron density is submitted in double logarithmic scale as a function of pressure in Fig. 4 [62]. One can see that the electron density rises from about 5×10^{13} cm^{-3} at $p =$ 30 torr up to 3.5×10^{15} cm^{-3} at pressure of 1500 torr.

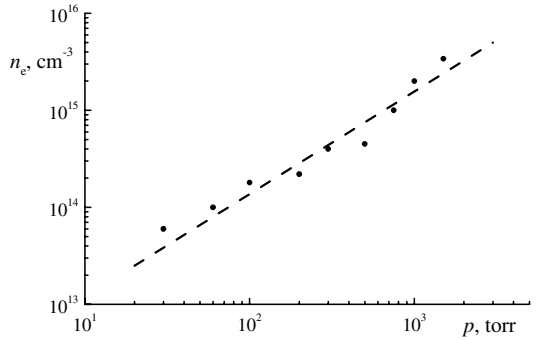

Fig. 4 Comparison of the experimental (points) electron density dependence on gas pressure in the plasma of a freely localized microwave discharge in air with the calculated values (dashed line) [65].

It was shown that a freely localized microwave discharge was not blown off by a supersonic flow from the focal region of a focused microwave beam, and the power required for producing a microwave discharge depended only slightly on the flow velocity. Thus, there was almost no difference between the situation in which a freely localized microwave discharge was initially excited in still air and then a supersonic flow was switched on, and the opposite situation in which a supersonic flow was initially switched on and then a microwave discharge was produced in the flow [19,26]. Note that, under our experimental conditions, the gas flow velocity was much lower than the discharge propagation velocity and the supersonic airflow with a Mach number of $M = 2$ only slightly affected gas heating. To confirm the hypothesis that plasma may be produced ahead of a body moving with a supersonic velocity in the dense atmosphere, we carried out experiments in which a microwave discharge was produced ahead of a model of the aircraft forepart flowed around by supersonic airflow at pressures of $p = 50$–500 torr. It was shown [19,26] that the generation of a discharge in a focused microwave beam is a reliable method for remotely controlling the production of plasma in a specified spatial region ahead of an aircraft moving with a supersonic velocity in the dense atmosphere.

B. Surface Microwave Discharge

The air pressure dependence of the minimum microwave breakdown power at which the discharge is initiated on the surface of the insulator is shown in Fig. 5. It can be seen that the power of the generator initiates the surface microwave discharge in a wide range of air pressures (from 10^{-3} to 10^3 torr). With increasing air pressure, the minimum discharge-initiating power first decreases and then increases. Such a dependence is similar to the Paschen curve and is explained by the fact that diffusion electron losses decline and inelastic electron losses increase when the pressure grows. To compensate for electron losses, a high ionization frequency is necessary, ionization frequency $\nu_i = f(T_e)$ grows with electron temperature, that is, with reduced electric field E/n or microwave power W. It was also shown [46] that, at a constant air pressure, the discharge-initiating power for $\tau = 1.5$–10 μs drastically drops, whereas, for $\tau > 50$ μs, the breakdown threshold is almost independent of the pulse duration.

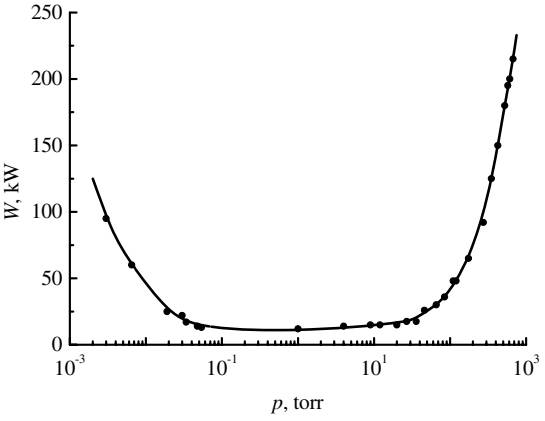

Fig. 5 Minimum microwave pulse power necessary for initiating the surface microwave discharge versus pressure at $\tau = 1.5$ μs and $f = 40$ Hz.

Assume that the external field is switched on much faster than the charged particles are generated and remains constant during the avalanching time. Under this assumption, we can suppose that, after the field has been switched on at zero time $t = 0$, the rates of ionization ν_i, attachment ν_a, and diffusion ν_D are time-independent, that is, $\nu_i(t)$, $\nu_a(t)$, and $\nu_D(t) = \text{const}$. Then, from the balance equation for the electron concentration, it follows that the following relationship is valid at impulse breakdown:

$$\nu_i = \frac{1}{\tau}\ell_n \frac{n_e}{n_{e0}} + \nu_a + \nu_D \qquad (1)$$

Here, the first term on the right of the equation takes into account the effect of pulse duration finiteness on the breakdown characteristics, n_e is the electron concentration, and n_{e0} is the concentration of seed electrons.

At low gas pressures ($p < 1$ torr), diffusion coefficient $D \sim l/p$ is large and electron losses due to diffusion ν_D/ν_a are high. To compensate for the losses, a very high ionization rate, that is, a very strong field, is necessary. At high pressures, diffusion electron losses are insignificant, so that even a field that is not too high (low ionization rate) might seem to be sufficient for breakdown. However, in this case, electron losses due to attachment become a key factor. The fact is that these losses limit the ionization rate. Let us evaluate the ionization rate for $p > 10$ torr, $\tau = 50$ μs, $n_{e0} = 10^2$ cm^{-3}, and $n_e = 10^{12}$ cm^{-3}. In this case, the attachment rate is higher than the diffusion rate. The first and second terms on the right of Eq. (1) are roughly equal to $4 \cdot 10^5$ and $6 \cdot 10^5$ s^{-1}, respectively, that is, their sum equals 10^6 s^{-1}. Therefore, the ionization rate at $p = 10$ torr must be equal to, or greater than, 10^6 s^{-1}, and at $p = 760$ torr, greater than $\sim 5 \cdot 10^7$ s^{-1}. Thus, calculation of the breakdown threshold at $\tau < 50$ μs must take into account the microwave pulse duration.

In the plasma space, a number of processes occur, such as gas heating, excitation of the vibrational degrees of freedom of the molecules, increase in the density of long-lived metastable electron-excited states, accumulation of charged particles (electrons and also positive and negative ions), variation in the chemical composition of the gas, and others. Basically, they may change the conditions for gas secondary breakdown. In particular, when the discharge is initiated in air by a train of pulses, the air heats up for the pulse time to a significant temperature, depending on the pulse power and duration. If the pulse repetition period is shorter than the characteristic cooling time of the air, the air has no time to cool down to the ambient temperature before the next pulse arrives. The discharge space is a region with a lower air density, $n < n_0$ (where n_0 is the density of the ambient air). In this case, a lower external field (microwave power) should be applied to reach the breakdown intensity of reduced electric field $(E/n)_b$.

Figure 6 shows the general view of the surface microwave discharge initiated on the wedge-nose dielectric antenna in air. It is seen that the discharge is localized in a thin surface layer. At this, the area covered by the wave-initiated plasma increases with the pulse

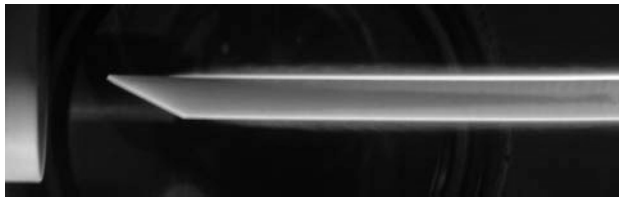

Fig. 6 Surface microwave discharge on the wedge-shaped dielectric antenna in air at $p = 40$ torr, $W_p = 40$ kW, and $\tau = 75$ μs.

duration and microwave power. When the microwave power or pulse duration was increased above the value necessary for the surface of the wedgelike antenna to be fully covered by the plasma, a new type of microwave discharge, namely, the combined surface and volumetric microwave discharge, emerged [47]. This phenomenon is a combination of a microwave discharge initiated on the surface of the wedgelike antenna and a space microwave discharge produced at its front edge. The size of a volume plasma object increases with pulse duration and microwave power. Our calculations show that, when the antenna is covered by the plasma incompletely, the coefficient of energy reflection from its front end is no higher than 0.15. If the discharge occupies the entire surface, the coefficient of reflection from the front end of the antenna may reach 0.85. In this case, a standing wave arises on the antenna surface with the typical spatial modulation of the plasma glow. From the discharge pattern observed, one can estimate the electron concentration in the plasma.

Studying the evolution of the surface microwave discharge, we found that, in the entire pressure range, the longitudinal length of the discharge increases with the microwave pulse duration and power delivered to the antenna. As an example, Fig. 7 shows the log-log plot of the longitudinal velocity of surface discharge propagation versus time at $p = 10$ Torr. The surface discharge propagation velocity is seen to increase with the applied power. Initially, this velocity is high, reaching $v_d = 10^7$ cm/s at a microwave pulse power of 175 kW. Subsequently, the discharge propagation velocity drops to $v_d = 10^4$ cm/s at $W_p = 25$ kW. It also follows from Fig. 7 that all the straight lines have the same slope. Similar results were obtained at different air pressure. It turned out that the experimental time dependence of the longitudinal velocity of the surface discharge is fitted well by the law

$$v_d = At^{-(0.875\pm0.035)} \tag{2}$$

where A is a power-dependent coefficient and t is the time. At air pressures $p = 10$–100 torr, coefficient A is directly proportional to W/W_0, where W_0 is the threshold power necessary for initiating a surface discharge at a given gas pressure. Using the relationship $A = f(W)$, one can derive the length of the surface discharge as a function of the microwave power,

$$L = 17\frac{W}{W_0}t^{(0.125\pm0.035)} \tag{3}$$

where L is the length of the discharge in centimeters and t is the time in seconds. This formula implies that our setup can initiate a surface microwave discharge of length up to $L \sim 1$ m.

The experimental results show that the velocity of discharge propagation over the surface of the dielectric antenna exceeds the velocity of sound in air, but is much lower than the electromagnetic wave velocity in free space. To explain such a value of the discharge propagation velocity, it is appropriate to compare it with the ionization rate for gas molecules, that is, with the critical concentration of electrons at the front of the discharge. To answer the question of whether discharge propagation mechanisms at the stages of discharge formation and evolution are different, let us see how the velocity of the front of the discharge varies with the surface discharge length. To this end, we construct a log–log plot of the discharge propagation velocity along the dielectric antenna versus longitudinal coordinate x. The associated curves $v_d = f(x)$ are shown in Fig. 8. These curves exhibit a characteristic kink, which indicates that different mechanisms are responsible for the propagation of the discharge at its initial and final stages.

Initially ($t = 1$–3 μs), the velocity of surface microwave discharge propagation in the discharge initiation region of the antenna (this region is bounded by coordinates $x = 1$ cm and $x = 2$ cm, i.e., is adjacent to the waveguide, which delivers the microwave energy to the antenna) exceeds 10^6 cm/s. Such a high discharge velocity in the region of electromagnetic energy delivery can only be provided by a mechanism associated with the breakdown wave. The motion of the surface discharge by the slow combustion mechanism is only possible late ($t > 100$ μs) in the discharge, when its propagation velocity becomes smaller than the velocity of sound. The most plausible mechanism of discharge propagation at a low gas pressure is ambipolar diffusion, whereas the photoionization and/or electronic heat conduction can control the discharge propagation only at a high pressure.

If ambipolar diffusion is the basic mechanism responsible for the loss of charged particles in plasma, the dependence of discharge propagation velocity v_d on ionization rate ν_i is given by

$$v_d = 2\sqrt{D_a\nu_i} \tag{4}$$

where

$$D_a = \frac{b_i kT_e}{e} \tag{5}$$

is the ambipolar diffusion coefficient, k is the Boltzmann constant, and b_i is the ion mobility. In air, the ion mobility is expressed as [63]

$$b_i p = \frac{2.7\sqrt{1 + M_g/M_i}}{\sqrt{(\alpha/a_0^3)29\cdot 10^{-3}}} \tag{6}$$

Here, p is the gas pressure in torr and $\alpha/a_0^3 = 11,54$. For the microwave breakdown of air, Mayhan [64] derived the following dependence of the ionization frequency on the reduced electric field:

$$\frac{\nu_i}{p} = 8.35\cdot 10^{-4}\left(\frac{E_{\text{eff}}}{p}\right)^{5.34} \tag{7}$$

where E_{eff} is the effective field, which is related to amplitude E_0 of the electric field intensity as

$$E_{\text{eff}} = \frac{E_0}{\sqrt{2}}\frac{\nu_{\text{en}}}{\sqrt{\nu_{\text{en}}^2 + \omega^2}} \tag{8}$$

Here, $\omega = 2\pi c/\lambda$ is the circular frequency of the microwave field, $\lambda = 2.4$ cm, and $\nu_{\text{en}} = 5.3\times 10^9 p$ is the frequency of electron-neutral collisions.

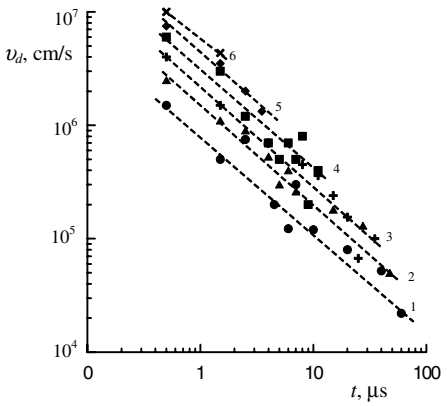

Fig. 7 Longitudinal propagation velocity of the surface microwave discharge versus time at $p = 10$ torr and $W_p =$ (1) 25, (2) 35, (3) 55, (4) 75, (5) 100, and (6) 175 kW.

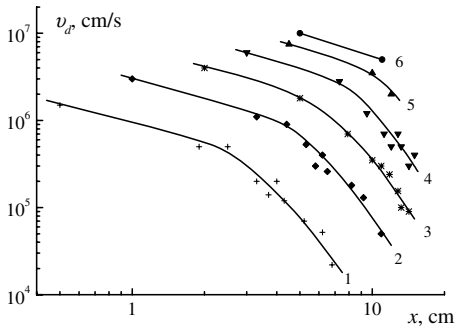

Fig. 8 Propagation velocity of the discharge versus the longitudinal coordinate at $p = 10$ torr and $W_p =$ (1) 25, (2) 35, (3) 55, (4) 75, (5) 100, and (6) 175 kW.

Using Eqs. (4–8), we find that, at air pressure $p = 10$ torr, the amplitude of the electric field intensity and the velocity of surface microwave discharge propagation are related as

$$E_0 = 45.3 \cdot \upsilon_d^{0.375} \tag{9}$$

where the electric field intensity is expressed in units of volts per centimeter and the velocity in meters per second.

Figure 9 demonstrates the semilog x dependences of the electric field peak intensity at the front of the propagating surface discharge. The curves were constructed for an air pressure of 10 torr using the measured velocity of discharge propagation along the antenna. Here, the applied microwave power serves as a parameter. Extrapolating these functions to $x = 0$, we find that, under the conditions of our experiment, the amplitude of the electric field intensity at the front of the surface microwave discharge near the waveguide edge changes from 2 kV/cm at pulse power $W_p = 25$ kW to ~5 kV/cm at $W_p = 175$ kW. It should be noted that the results obtained are in good agreement (rather than in conflict) with the field in the waveguide calculated by the formula

$$E_0 = 28\sqrt{S} \tag{10}$$

where power flux density S is expressed in watts per square centimeter, nd amplitude E_0 of the electric field intensity in volts per centimeter. For example, at applied pulse power $W_p = 175$ kW, the electric field amplitude in the waveguide is $E_0 \sim 8$ kW/cm; at $W_p = 25$ kW, the field amplitude is ~3 kV/cm.

The analytical results obtained for high pressures distinctly contradict the experimental data. Particularly, at a pressure of 100 torr, the electric field amplitude in the surface discharge calculated in the ambipolar diffusion approximation $E_0 = 259\upsilon_d^{0.375}$ reaches 15 kW/cm. This value is obviously different from the waveguide field found experimentally.

Next, suppose that the discharge propagation is governed by electronic heat conduction. In this case, the discharge velocity depends on the electric field intensity as

$$\upsilon_d = \frac{\sqrt{\chi_e \sigma T_e}}{(3/2)kT_e n_e} E_0 \tag{11}$$

where $\chi_e = 2.56 \times 10^{-2} T_e^{5/2} / \ell_n \Lambda$ is the electron thermal conductivity in W/(cm · K), σ is the electron conductivity, and T_e is the electron temperature in electron volts. In air, $\chi_e = 1.93$ W/(m · K), $\sigma p / n_e = 7.21 \times 10^{-18}$ torr · m^2/Ω [63]. Finally, we obtain

$$E_0 = 1.46 \times 10^{-5} \sqrt{p} \upsilon_d \tag{12}$$

where the velocity is expressed in meters per second, the pressure in torr, and the electric field intensity in volts per centimeter.

At pressure $p = 100$ torr and discharge propagation velocity $\upsilon_d = 10^5$ m/s, the maximal field amplitude calculated under the assumption that the discharge propagates by the mechanism of electronic heat conduction equals 14.6 V/cm. Such a value of the field amplitude disagrees with the experimental data, and, hence, the mechanism of electronic heat conduction cannot maintain the discharge throughout the pressure range studied.

The basic properties of the surface microwave discharge created on an external surface of the dielectric antenna at low air pressure $p < 1$ torr under conditions when the frequency of collisions of electrons with molecules were less than the circular frequency of an electromagnetic field were also considered. With the pulse duration fixed, the transversal size of the surface microwave discharge decreases at an increase in the air pressure. As an example, the received results are submitted in Fig. 10 at air pressure $p = 0.5$ torr. It is visible that longitudinal speed of the discharge propagation strongly (in conditions of the experiment on 2 orders of value) changes during microwave pulse duration, whereas transversal speed of distribution of the surface microwave discharge remains practically constant, decreasing to the end of a pulse only 3 times. Thus, at the initial stages of development of a surface microwave discharge, the longitudinal speed exceeds the transverse one by more than an order of magnitude, and at the late stages of discharge existence, the longitudinal and transversal speeds are equal to each other with a good degree of accuracy. These facts specify that, at late stages of longitudinal and transversal development of the discharge, the same mechanism answers. It is obvious that, at low pressure of air, such mechanism can only be ambipolar diffusion.

The data on electron concentration were measured by the Stark broadening of the H_β ($\lambda = 486.1$ nm) line of hydrogen. It was obtained that the electron density at a distance of $y = 1$ mm from the antenna surface reaches a value of 10^{14} cm^{-3}. The electron concentration was determined also with the help of the probe method. Spatial distribution of electron density is submitted in Fig. 11. It can be seen that concentration of electrons in a narrow boundary layer, where the electric field of a surface wave is located, reaches a value of 10^{14} cm^{-3}. The transversal sizes of the plasma areola increase when air pressure decreases. As tentative estimations show, the processes of photoexcitation, photodissociation, and

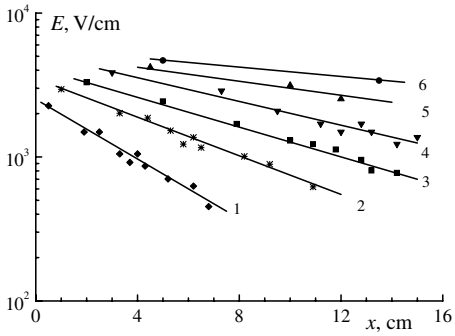

Fig. 9 Electric field amplitude at the front of the surface wave versus the longitudinal coordinate at air pressure $p = 10$ torr and $W_p =$ (1) 25, (2) 35, (3) 55, (4) 75, (5) 100, and (6) 175 kW.

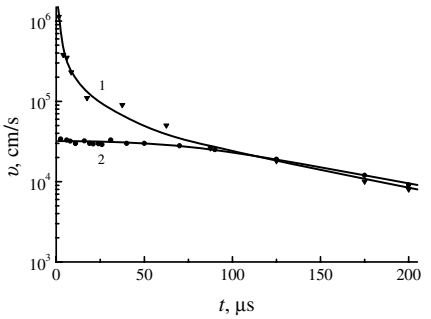

Fig. 10 Time dependencies of longitudinal (1) and transversal (2) velocities of the surface microwave discharge; $p = 0.5$ torr, $W_p = 35$ kW.

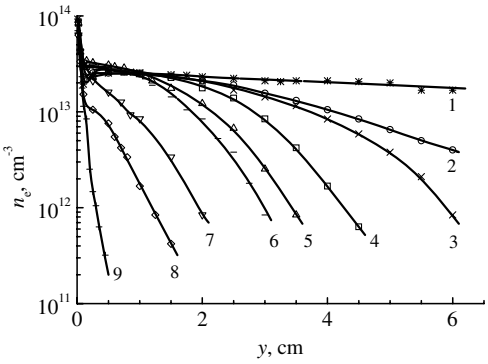

Fig. 11 Transversal distribution of electron density in plasma of a surface microwave discharge; $\tau = 100$ μs, $W_p = 55$ kW, p, torr: (1) 0.1; (2) 0.2; (3) 0.3; (4) 0.5; (5) 1; (6) 2; (7) 5; (8) 10; (9) 20.

photoionization of air bring the certain contribution to formation of the measured distribution of electron density.

Under conditions of a surface microwave discharge, effective dissociation molecules of oxygen and nitrogen takes place. Time dependence of the transversal sizes of area of localization of atomic excited oxygen, measured on a luminescence of a triplet line of oxygen ($\lambda = 777.1, 777.4$, and 777.5 nm), is submitted in Fig. 12. It is seen that the transversal sizes of localization of atomic excited particles practically coincide with the sizes of plasma measured by a probe method.

Longitudinal distributions of gas temperature at low air pressure and threshold values of an input microwave power were measured. It was shown that, with an increase of air pressure from 0.01 to 10 torr, the gas temperature increases from 300 to 1200 K, and, in the direction of the discharge propagation, the gas temperature decreases insignificantly. It was also shown that the longitudinal distribution of gas temperature smooths out when microwave power increases. It is defined that, with an increase in power, longitudinal speed of the discharge propagation grows, the discharge occupies the whole antenna length, thus there is an effective reflection ($R \sim 85\%$) surface wave from the forward end of the antenna. Under these conditions, the energy input to a gas in discharge on a unit of length of plasma is constant on the discharge length. It was also shown that, at a stage of the discharge formation, the gas heating rate grows with an increase of power (curve 1 in Fig. 13) and can reach a value of ~ 70 K/μs at $W_p = 200$ W. On a quasi-stationary stage of discharge existence (curve 2 in Fig. 13), a gas heating rate is equal to 10 K/μs and does not depend on power.

For numerical modeling, we used a nonstationary kinetic model that was used under conditions of a freely localized microwave discharge. Our calculation shows that the mechanism responsible for rapid gas heating is efficient generation of electron-excited states in nitrogen molecules at high values of the reduced electric field ($E/n > 10^{-15}$ V · cm^2), followed by quenching of these states. Part of the energy of these excited states is converted to heat, causing the rapid growth of the gas temperature observed in the experiment.

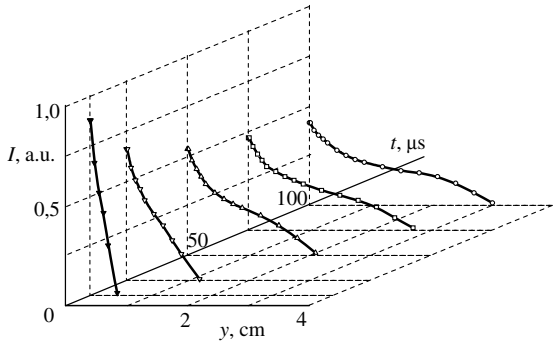

Fig. 12 Transversal sizes of area of excited atomic oxygen localization in plasma of the surface microwave discharge; $W_p = 55$ kW and $p = 0.5$ torr.

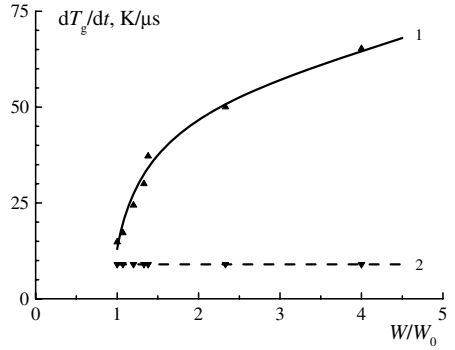

Fig. 13 Gas heating rate as a function of a microwave power. Initial phase (1) and stationary phase (2) of the discharge W_0 is threshold value of an input microwave power.

C. Microwave Plasma-Assisted Ignition

1. Ignition with Help of a Freely Localized Microwave Discharge

The possibility of controlling the ignition and combustion of the fuel in a hypersonic ramjet engine is an important condition for its practical use. In our experiments, we at first studied the influence of a nonequilibrium plasma of a freely localized microwave discharge on the combustion kinetics of a gaseous hydrocarbon fuel using the ignition of a supersonic propane-airflow with a Mach number of $M = 2$ as an example. When a microwave discharge was excited in still air inside the aerodynamic channel, a plasma 1–2 cm in size was produced near the initiator (Fig. 14a). The discharge dimensions were found to increase with increasing power and duration of the microwave pulse. Figures 14b and 14cshow photographs of freely localized microwave discharges in supersonic air and air–propane flows in the aerodynamic channel. It turned out that the supersonic flow of a gaseous hydrocarbon fuel was easy to ignite by a microwave discharge. In our experiments, the combustion of a supersonic air–propane flow was successfully initiated by microwave beams with a duration as short as $\tau = 25$ μs.

Besides photographing the general view of a discharge in the aerodynamic channel, we recorded the emission spectra from the combustion products of an air–propane mixture in different regions of the aerodynamic channel. Thus, in the case of a microwave discharge in a supersonic airflow, the emission spectrum measured at a distance of $z = 7$ cm downstream from the beam focus did not contain any atomic lines and molecular bands. In contrast, in the emission spectrum from a discharge in a supersonic air–propane flow, we observed intense radiation from the excited CH^* radicals, the molecular bands of C_2 and CN, and the spectral lines of atomic oxygen and hydrogen. In this case, the radiation pulse lasted over ~ 1 ms, whereas the duration of the microwave pulse initiating combustion was $\tau = 100$ μs.

It was known that, at high values of the reduced electric field ($E/n \geq 10^{-15}$ V · cm^2), a significant fraction (more than 50%) of the energy deposited in the discharge is spent on the excitation, dissociation, and ionization of molecules by electron impact with the subsequent generation of chemically active radicals. Because a self-sustained microwave discharge exists at high values of the reduced electric field [32], the number of active particles produced in such a discharge is larger than that in an electrode discharge. This should strongly affect the kinetics of the processes with the participation of active radicals, and should result in a shorter induction time. Our experiments indicate [19–47] that, at high values of the reduced electric field, the gas in a microwave discharge is rapidly heated ($dT_g/dt \sim 10^8$ K/s) and the degree of molecular dissociation is high (up to $\delta \sim 50\%$); this promotes the rapid fuel ignition. It should be noted that, because the reduced electric field in a microwave

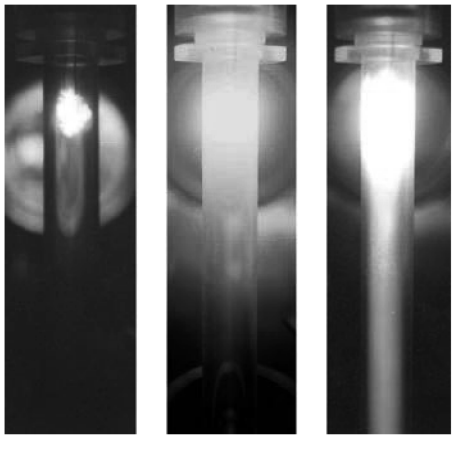

Fig. 14 General view of a freely localized microwave discharge produced in a) still air at a microwave power of $W_p = 100$ kW, and in supersonic ($M = 2$) b) air and c) air–propane flows at $W_p = 200$ kW. Static air pressure in the chamber is $p = 60$ torr, and the microwave pulse duration is $\tau = 100$ μs.

discharge is high, the plasma is a source of intense UV radiation, which may substantially affect the production of active radicals via photoionization, photodissociation, and photoexcitation. This is also favorable for reducing the induction time. For this reason, we believe that it is necessary to more thoroughly examine the role of charged and active particles, which are very rapidly produced in a microwave discharge, and the influence of UV radiation on both the reduction of the induction time and the increase in the combustion efficiency of hydrocarbon mixtures.

2. *Ignition with Help of a Surface Microwave Discharge*

The typical integrated photos of the surface microwave discharge in supersonic flow of air (a) and propane–air mixture (b) are resulted in Fig. 15. One can see that the discharge in air represents uniformly brightly luminous plasma coating the surface of a dielectric body. However, it is necessary to also note that, in a photo, it is visible weakly luminous "halo," existing around antenna. From here it is possible to conclude, that this low-density plasma arises due to photoionization of impurity molecules own ultraviolet radiation of plasma of a surface microwave discharge. The surface microwave discharge exists at large values of an electric field and electric field is located in thin ($d < 1$ mm) near-surface layer. It results in effective excitation of high-energy levels of molecules and atoms with the subsequent generation of ultraviolet radiation causing photoionization of impurity molecules. This phenomenon can play the important role at use of a surface microwave discharge for assistant combustion of supersonic streams of hydrocarbon fuels.

Under condition of surface microwave discharge in propane airflow (Fig. 15b) the characteristic luminescence of a flame in a supersonic stream (see Fig. 15b) is observed. Thus speed of burning front distribution reaches values of 100–200 m/s depending on energy put in the surface microwave discharge. At this the place of the greatest burning localization occurs in a zone of the beginning of the dielectric antenna where intensity of electric field is maximal. Such spatial distribution of front of burning of a supersonic stream of a propane–air mixture confirms our assumption of the large contribution of own ultraviolet radiation of a surface microwave discharge in kinetics of ignition and burning hydrocarbon fuels. It is necessary to note that process of burning stops with the ending of the microwave pulse duration.

The spectrum of radiation in the diapason of wavelengths $\lambda =$ 350–425 nm was also recorded. Spectroscope was adjusted on the area of the antenna located on distance $x = 2.5$ cm from the supply waveguide. It was received, that in this spectrum area the intensive bands of the second positive system of nitrogen and bands of CN are observed. In case of supersonic stream of air the gas temperature measured by various molecular bands is equal 800–1000 K. At ignition of a propane–air supersonic stream the general view of a spectrum in this area of wavelengths essentially varies, namely, intensity of a luminescence of CN bands sharply grows, whereas intensity of a luminescence of bands of the second positive system decreases. The gas temperature measured by CN bands, sharply grows. In this case $T_g = 2750$ K, that also testifies to ignition of supersonic stream of gaseous fuel on an external surface of a plate. At $W_p = 40$ kW the induction period $\tau_{ig} \approx 30$ μs. At a pulse microwave power of 60 kW, ignition of a propane–air mixture occurs faster than at $W_p = 40$ kW. The intensity of CH luminescence in some times exceeds the intensity of a luminescence in air. Thus, the luminescence already starts to grow sharply during the first moments ($t = 3$–5 μs) of microwave energy action.

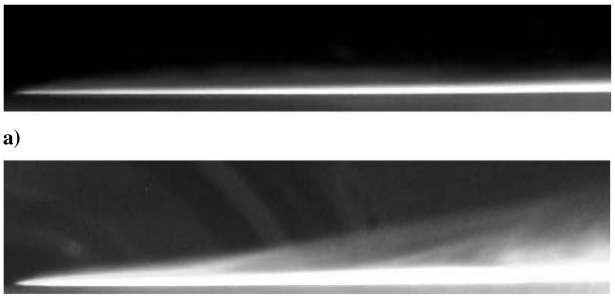

a)

b)

Fig. 15 Side view of a surface microwave discharge on the top part of the flat antenna streamlined by supersonic stream of a) air and b) propane–air mixtures at $M = 2$, $p = 40$ torr, $\tau = 100$ μs, $W_p = 40$ kW, $p_{air} = 1$ atm, and $p_g = 4.5$ atm.

3. *Ignition with Help of a Transversal Pulsed-Periodic Electrode Discharge*

In Figs. 16 and 17, the common view of the pulse-periodic transversal surface discharge in the aerodynamic channel are represented at various depths of a stagnant zone. One can see that the transversal surface discharge represents two smooth plasma jets extended along a stream in the aerodynamic channel without a stagnant zone (Fig. 16). In wind tunnels, the volumetric transversal discharge has the same structure. It testifies to uniformity of a supersonic stream in our channel without a stagnant zone. The discharge structure starts to vary sharply at its creation in a cavity. Stream turbulization is observed. At the depth of a stagnant zone $h = 3$ mm (Fig. 17), there are the opposite separated currents and the discharge goes in two directions, both upstream and downstream. The recirculation area with a vortex movement about a forward wall of a stagnant zone is formed. At the use of a stagnant zone at depth $h = 5$ mm, the discharge exists only about a forward wall of a cavity and is not spread downstream. These circumstances are promising from the point of view of use of a cavity as a source of the active particles, promoting fast ignition and stable burning of a supersonic stream of a gas mixture.

Probe current and typical temporal behavior of CH^* emission is given in Fig. 18 under the condition of a propane–air mixture ignition. One can see that, as well as an optical method, the probe method is a reliable way of diagnosing the process of combustion of a propane–air mixture. It was experimentally shown that a stagnant zone results in stabilization of combustion of a supersonic propane–air mixture. For example, even a stagnant zone at a depth of 2 mm can result in a sharp increase of combustion time, up to 1000 μs at discharge pulse duration $\tau = 200$ μs.

4. *Stabilization of Propane–Air Combustion in Aerodynamic Channel with a Cavity*

As a stagnant zone in experiments, the rectangular cavity with different lengths L to depth h ratio ($L/h = 1$–10) was used. A cavity has allowed us to use a direct-current power supply unit with voltage

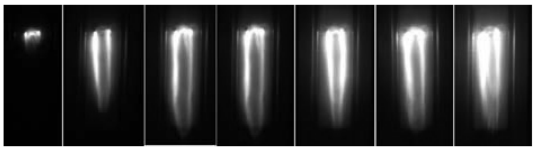

1 2 3 4 5 6 7

Fig. 16 Pulse-periodic transversal surface discharge in supersonic airflow with $M = 2$ in the aerodynamic channel of rectangular section 10×18 mm^2 without stagnation zone ($h = 0$ mm); front view. The supersonic airflow is directed from top to bottom. $p = 150$ torr, $p_0 = 2$ atm, $i = 8$ A, τ, μs: (1) 100, (2) 200, (3) 300, (4) 400, (5) 600, (6) 800, and (7) 1000.

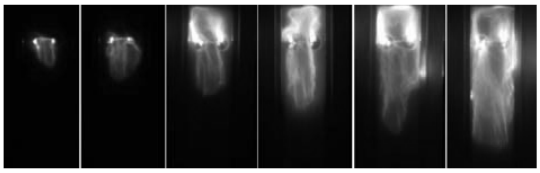

1 2 3 4 5 6

Fig. 17 The same as Fig. 16, with $h = 3$ mm, τ, μs: (1) 75, (2) 150, (3) 300, (4) 600, (5) 800, and (6) 1000.

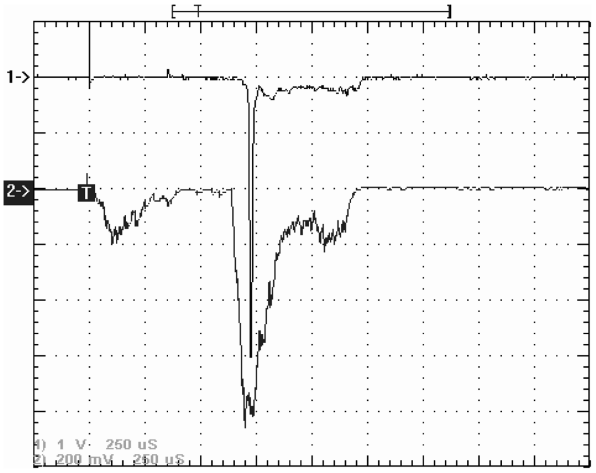

Fig. 18 Ignition of the supersonic propane–air mixture at $p = 150$ torr, $p_{air} = 2$ atm, $p_g = 5$ atm, $i = 16$ A, $\tau = 350$ μs. Probe (1) located at the distance $z = 32$ cm downstream from electrodes. The area of the aerodynamic channel, from which the CH* emission (2) was registered, located at the distance $z = 30$ cm downstream from electrodes.

$U = 2.5$–4.5 kV for creation of the surface discharge. With the help of this power supply unit, it is impossible to create the discharge in freestream or the surface discharge in the channel without a stagnant zone, as its voltage is not enough for maintenance of the discharge in supersonic flow. However, this power supply unit allows one to support the surface electrode discharge in a cavity during time $t = 1$–2 s. The low-current, high-voltage pulsed source was used for breakdown of a discharge gap. The typical temporal behavior of CH* emission, discharge current, and voltage on the discharge gap is represented in Fig. 19 at use of a transversal surface electrode discharge in a stagnant zone in the aerodynamic channel for combustion of the supersonic propane–air mixture. One can see that, after breakdown, the voltage on the discharge gap quickly reduces from 4.5 kV to 250 V. At this, there is a time delay of stationary combustion of propane–air mixture achievement. Under experimental conditions, the time delay is about 400 ms.

The time t_1 of the beginning of process of burning and time t_2 of an achievement of stationary burning of a propane–butane–air mixture as a function of discharge current were measured. Time of the beginning of process of burning of supersonic propane–airstream was defined as a time interval from gas breakdown and forming of the discharge up to achievement of signal from the photo electronic multiplier, recording intensity of radiation of CH band of level $I_1 = 0.1 \times I_{st}$, and time of achievement of stationary burning was determined on achievement of intensity of a luminescence of level $I_2 = 0.9 \times I_{st}$. It was shown that rate of ignition increases with growth of discharge current, thus the stationary mode of burning is established faster. So at small discharge currents ($i < 10$ A), that is, at small electric powers ($W < 2$ kW), the burning begins only by the end of a pulse duration of 750 ms, whereas, at the large discharge currents ($i \sim 30$ A, $W \sim 6$ kW), the stationary mode of burning is achieved through 150–200 ms.

Process of fuel ignition strongly depends on structure of a combustible mixture. Time evolution of ignition of a supersonic combustible mixture was measured at different percentages of gas in a mixture at a constant amount of air and at the constant of gas consumption and change of the air consumption. All measurements were carried out at discharge current $i = 8$ A. Results of processing of the received data are submitted in Fig. 20. One can see that, both in the case of a poor mixture and in the case of an enriched mixture, an achievement time of combustion stationary mode increases in comparison with a stoichiometric mixture.

It is necessary to note that, in our conditions, in the case of the powerful high-voltage pulsed power supply used for ignition, the induction time equals hundreds of microseconds, whereas, at use of low-voltage power supply, the induction time grows sharply. This fact indirectly confirms our assumption about the strong influence of the charged and active particles, formed in the discharge at large values of reduced electric field, on process of ignition of supersonic gaseous fuels.

5. Combustion of Propane–Airflow Under Condition of Combined Microwave Discharge

We have also fulfilled experiments on the use of an intensification and stabilization of a supersonic propane-airstream combustion of the combined microwave discharge created in various stagnant zones of the aerodynamic channel. It was shown that the combined microwave-dc discharge in a stagnant zone behind the reverse step of the aerodynamic channel results in fast ignition and combustion of propane–airflow. However, efficiency of combustion of a supersonic stream of hydrocarbon fuel was not so good. Under these conditions, the flame does not pass in the basic stream. Under condition of the combined microwave-dc discharge, created in a rectangular cavity, efficiency of burning increases in comparison with a case of creation of the discharge in a stagnant zone behind a reverse step. The result of supersonic combustion of the propane-airstream, received at the use of a rectangular cavity with angled rear-wall on a wall of the aerodynamic channel as flame stabilizers and flame holders, is submitted in Fig. 21. Received results testify to efficiency of the use of combined microwave discharge in supersonic aerodynamics. However, it is necessary to find optimum modes of creation of the discharge and optimum configurations of the aerodynamic channel for stabilization of supersonic combustion and increase completeness of the combustion of hydrocarbon fuel.

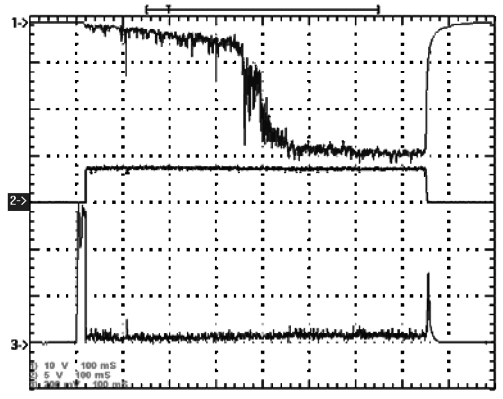

Fig. 19 Combustion of the supersonic propane–air mixture in the aerodynamic channel. Transversal surface discharge in a stagnant zone $h = 17$ mm, $L = 70$ mm, $p = 150$ torr, $p_{air} = 2$ atm, $p_g = 4$ atm, $M = 2$, $i = 12$ A, $U_d = 250$ V, $\tau = 750$ ms, $m_g = 4,4$ g/s, $m_{air} = 70$ g/s; (1) typical temporal behavior of CH* emission; (2) discharge current; (3) voltage on discharge gap.

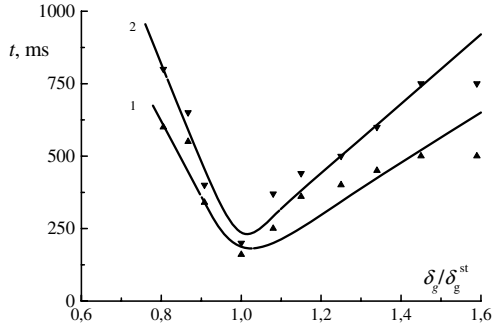

Fig. 20 Time of the beginning of occurrence of burning (curve 1) and time of achievement of stationary burning of a propane–air mixture (curve 2) as a function of air consumption. $M = 2$, $\tau = 750$ ms, $U_d = 250$ V, $h = 17$ mm, $L = 70$ mm, $p = 150$ torr, $i = 8$ A, $p_g = 4.05$ atm, $m_g = 4.35$ g/s, $p_0^{st} = 2$ atm, $m_{air}^{st} = 70$ g/s.

Fig. 21 Combustion of a supersonic ($M = 2$) propane-airstream at use for ignition and burning stabilization, the combined microwave discharge created in aerodynamical channel with a rectangular cavity with angled rear wall at microwave pulse duration $\tau = 10$ μs, repetition frequency $f = 100$ Hz, duration of dc current $t = 1$ s, time exposure is 20 ms. The supersonic air–propane flow is directed from right to left.

V. Mathematical Modeling

A numerical model has been developed to study C_3H_8–air thermal autoignition by near-wall heat deposition. Computations have been performed for supersonic flow of a stoichiometric propane–air mixture over a blunted flat plate length of 15 cm and thickness of 0.02 cm for freestream velocity of 519 m/s, pressure of 98 torr, and temperature of 167 K. The gas-phase model involving 30 species ($C_3H_8, O, H, O_2, N_2, H_2, CO, OH, H_2O, HO_2, H_2O_2, HCO, CO_2, CH, CH_2, CH_3, CH_4, C_2H, C_2H_2, C_2H_3, C_2H_4, C_2H_5, C_2H_6, C_3H_5, C_3H_6$, i-C_3H_7, n-C_3H_7, CH_2O, CH_2OH, CH_3OH) and 70 chemical reactions was employed to describe the ignition process. An adiabatic, full noncatalytic model of gas-wall thermal and chemical interactions was used. Calculations were carried out in conditions similar to experimental conditions on creation of the surface microwave discharge. It was assumed that heat is deposed during time period of 100 μs with constant total power $P_d = 2500$ W/cm uniformly into the near-wall region $0.5 \le x \le 15$ cm, $0 \le y \le 0.1$ cm. The heat supply is started into an initially steady-state turbulent stream.

Figures 22–24 show the time history of predicted gas temperature, wall C_3H_8 mole fraction, and wall CO_2 mole fraction distributions along the plate surface. Presented in Figs. 22–24, data indicate that, for the considered conditions, ignition of the fuel mixture occurs after ending of heat supply pulse at a distance of about 4 cm from the plate heading. By this time, the gas temperature near the wall reaches ~3000 K. After ignition, front burning moves downstream at a rate of about 300 m/s. Temperature of the gas decreases and completeness of combustion increases. In the gas mixture behind the front, fractions of final combustion products H_2O and CO_2 rise, whereas fractions of oxygen and intermediate products of combustion drop.

Numerical analysis has shown that, for shorter heating pulse or smaller heating power, when temperature is not achieved to a value of ~3000 K, ignition does not occur. These results contradict the experimental data (executed at the same initial conditions) which

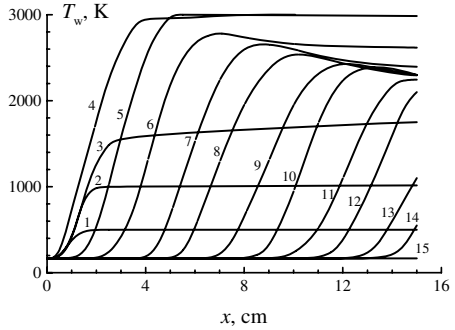

Fig. 22 Time history of wall temperature distribution; t, μs: (1) 25, (2) 50, (3) 75, (4) 100, (5) 150, (6) 200, (7) 250, (8) 300, (9) 350, (10) 400, (11) 450, (12) 500, (13) 550, (14) 600, (15) 650.

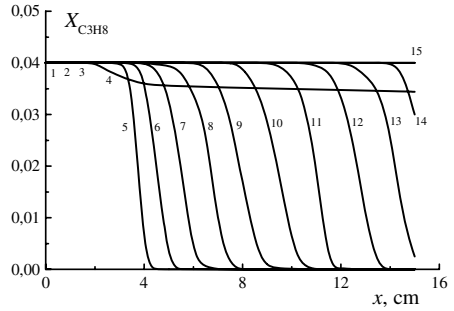

Fig. 23 Time history of wall C_3H_8 mole fraction distribution; t, μs: (1) 25, (2) 50, (3) 75, (4) 100, (5) 150, (6) 200, (7) 250, (8) 300, (9) 350, (10) 400, (11) 450, (12) 500, (13) 550, (14) 600, (15) 650.

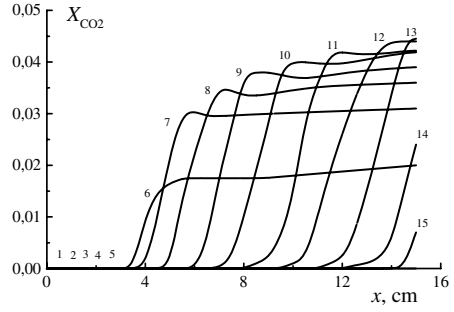

Fig. 24 Time history of wall CO_2 mole fraction distribution; t, μs: (1) 25, (2) 50, (3) 75, (4) 100, (5) 150, (6) 200, (7) 250, (8) 300, (9) 350, (10) 400, (11) 450, (12) 500, (13) 550, (14) 600, (15) 650.

show that ignition of a supersonic propane-airstream in the experiment occurs much faster ($t = 5$–25 μs) and at a smaller temperature ($T_g \sim 1000$ K) than at mathematical modeling. Connected to that fact is that, in calculations, the surface microwave discharge was considered as the source of thermal energy entered into a boundary layer, and plasma effects were not examined.

In the overwhelming majority of the executed experimental and theoretical researches, devoted to application of various types of gas discharges for ignition of fuels mixtures, the gas discharge was considered only as a source of thermal energy entered into system. However, the various gas ionization degrees are achieved for different types of gas discharges at the same applied specific power. At this, the electric energy input is differently distributed on internal degrees of freedom of molecular gas. This distribution is strongly dependent on the reduced electric field which, in turn, is determined by electrodynamics of the discharge. The different result can be received at the same power of energy source. For example, for ignition of a supersonic propane-airflow with Mach number $M = 2$, we used a dc electrode discharge, pulse-periodic transversal electrode discharge, freely localized electrodeless microwave discharge, and surface microwave discharge. The induction period as a function of reduced electric field under these conditions is presented in Fig. 25. The ignition of a propane–air mixture with the help of the surface microwave discharge had taken place already at pulse duration $\tau = 5$–20 μs, whereas, in the same conditions, the pulse-periodic transversal electrode discharge resulted in ignition only at $\tau \ge 150$–200 μs. It testifies that, in plasma of a microwave discharge, there are more charged and active particles than in plasma of the pulse-periodic electrode discharge. Therefore, from our point of view, it is necessary to investigate in detail the influence of the charged and active particles on reduction of an ignition delay and on increasing of completeness of propane–air mixture combustion.

The kinetic model was worked out by us for finding the influence of different channels on ignition of combustible mixtures. For example, mathematical modeling was fulfilled for a motionless hydrogen–oxygen mixture. To define the influence of various channels on ignition of a gas mixture, the kinetic model, including 29

components and 241 direct and reverse reactions, has been developed [26]. Such components, as neutral, not excited particles (H_2, O_2, H, O, OH, HO_2, H_2O_2, H_2O, O_3), the excited molecules of oxygen [$O_2(a)$, $O_2(b)$], positive ions (O^+, O_2^+, O_4^+, H^+, H_2^+, H_3^+, H_5^+, OH^+, H_2O^+, H_3O^+, $O_3H_2^+$), negative ions (O^-, O_2^-, O_3^-, O_4^-, H^-, OH^-), and electrons (e) were considered at modeling.

The system of the equations describing processes of oxidation in such mixtures and including the equation for energy, the equation for concentration of particles, and the equation of state have been put in the basis of model:

$$\frac{dH}{dt} = 0, \qquad H = N \cdot \sum_{i=1}^{M_1} \gamma_i \left(h_{0i}[T_0] + \int_{T_0}^{T} C_{Pi}\, dT \right)$$

$$\frac{d\gamma_i}{dt} = G_i - \gamma_i \sum_{k=1}^{M_1} G_k, \qquad G_i = \sum_{q=1}^{M_2} \frac{\alpha_{iq}^- - \alpha_{iq}^+}{N} [R_q^+ - R_q^-]$$

$$R_q^{\pm} = k_q^{\pm} \prod_{j=1}^{n_q^{\pm}} (N\gamma_{n_{jq}^{\pm}})^{\alpha_{jq}^{\pm}}, \qquad \frac{dN}{dt} = N \sum_{k=1}^{M_1} G_k$$

where γ_i is the mole fraction of corresponding component i, N (mol/cm^{-3}) is the total concentration, c_{pi} is the molar heat capacity of species i at $p = \text{const}$, $h_{0i}[T_0]$ is the molar enthalpy of formation of species i at $T_0 = 298$ K, M_1 is the full number of components, $k_q^{\pm}$ is the rate constant with participation of species i, M_2 is the full number of such reactions, and α_{iq}^+ and α_{iq}^- are the stoichiometric coefficients. Decomposition

$$C_{Pi} = \sum_{a=1}^{6} C_{Pi}^{(a)} \left(\frac{T}{10^4} \right)^{a-1}$$

has been used for calculation of a thermal capacity. The rate constants of reactions can be found in [25] and the references therein.

Ignition of a hydrogen–oxygen mixture under conditions of nonequilibrium low-temperature plasma of the gas discharge, existing at high values of the reduced electric field, was calculated on the model, taking into account dissociation of molecules and creation of active radicals and charged particles. As the temperature of gas under conditions of the discharge grows at a rate of about 10^2 K/μs, it was considered that, at power-up, the gas temperature instantly increases up to some initial value T_0. Calculations were carried out without taking into account losses of energy and diffusion of active particles in surrounding space. Calculations have been executed at initial pressure $p = 0.1$ MPa for a stoichiometric H_2-O_2 mixture at a variation of initial gas temperatures $T_0 = 800$–1200 K, electron temperatures $T_e = 0.1$–1.6 eV, and fractions stoichiometric ϕ. Fractions stoichiometric ϕ is the ratio of consumption of hydrogen in the mixture to its share in the stoichiometric mixture $(\gamma_{H_2}/\gamma_{O_2})/(\gamma_{H_2}/\gamma_{O_2})_{st}$. The modeling of kinetics of autoignition of a hydrogen–oxygen mixture was fulfilled with the use of the kinetic scheme, including 9 components and 60 reactions. It was shown that creation of radicals takes place up to the moment of ignition. At initial temperature 900 K, the ignition occurs at time ~1 ms. At the initial stage ($t = 0$–1 ms), the gas temperature rises very slowly and then, during the moment of ignition, suddenly changes from initial temperature up to the final ~3000 K. Dependences of ignition time of a hydrogen–oxygen mixture on hydrogen consumption were calculated at various initial gas temperatures. It has been shown that induction time depends both on a ratio of mixture and from initial gas temperature. At that, with the growth of gas temperature, ignition time decreases at any ratio of components of a mixture. At the same time, at any gas temperature, the ignition time of a mixture grows both at increase and at reduction of a fraction of hydrogen in a mixture in comparison with a fraction stoichiometric $\phi = 1$.

The ignition of the hydrogen–oxygen mixture under the model, with the account of molecules dissociation and creation of active radicals and charged particles, at high values of reduced electric field, was calculated with use of the initial kinetic scheme, including 29 components and 241 reactions. For example, in Fig. 26, the time dependence of mole fractions at ignition of stoichiometric H_2-O_2 = 2–1 mixture under condition of nonequilibrium plasma of gas discharge is represented. The mechanism of ignition represented in Fig. 26 is distinct from the mechanism of autoignition of the hydrogen–oxygen mixture. So, for example, process of creation of radicals and active particles is essentially accelerated at the presence of the discharge, due to quantitative and qualitative changes from a simple formation of active radicals as a result of interaction of not-charged particles to a creation of active radicals as a result of interaction with the charged particles. As a consequence of this fact, the mechanism of ignition also varies. In this case, the creation of active components occurs generally due to the discharge. The rate of creation of radicals and the charged particles increases at the growth of reduced electric field E/n, that is, electron temperature T_e. This circumstance results in essential reduction in an induction time.

It was also shown that, with an increase in electronic temperature, that is, the reduced electric field, the ionization frequency grows sharply, at gas temperature $T_0 = 900$ K, a delay time of an avalanche development also decreases from ~200 μs at $T_e = 1.35$ eV up to ~0.5 μs at $T_e = 1.6$ eV. Thus, during development of an avalanche, not only concentration of the charged particles, but also concentration of radicals and active atoms grow sharply. At $T_e = 1.35$ eV, concentration of metastable molecules $O_2(a^1\Delta_g)$, $O_2(b^1\Sigma_g^+)$, atoms H and O, and also radicals on stages of an avalanche development increase for the order of value, whereas, at $T_e = 1.6$ eV, a jump of concentration of these particles reaches 5–6 orders of value. Naturally, it results in significant reduction of the

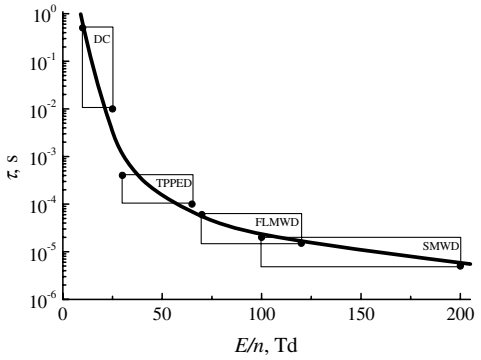

Fig. 25 Induction period as a function of reduced electric field. High-speed propane-airstream with Mach number $M = 2$. DC: direct-current electrode discharge; TPPED: transversal pulse-periodic electrode discharge; FLMWD: freely localized microwave discharge; SMWD: surface microwave discharge.

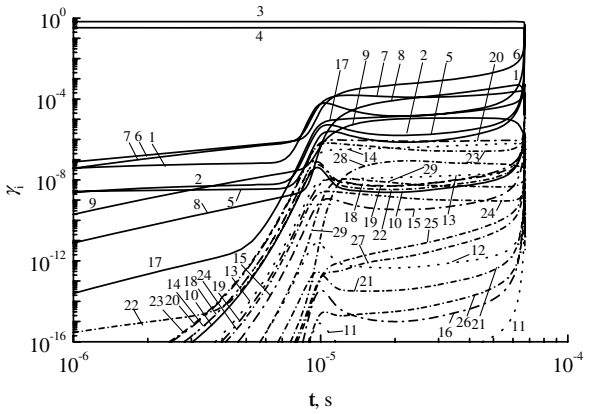

Fig. 26 Time dependence of mole fractions at ignition of stoichiometric H_2-O_2 = 2–1 mixture under condition of nonequilibrium plasma of gas discharge at $T_e = 1.4$ eV, $T_0 = 900$ K, $N_0 = 4.4 \times 10^{-5}$ mol/cm^{-3}. (1) H, (2) O, (3) H_2, (4) O_2, (5) OH, (6) H_2O, (7) HO_2, (8) H_2O_2, (9) O_3, (10) e, (11) H^+, (12) H_2^+, (13) H_3^+, (14) H_5^+, (15) O^-, (16) O^+, (17) $O_2(a^1\Delta_g)$, (18) O_2^-, (19) O_3^-, (20) O_4^-, (21) H^-, (22) $O_2(b^1\Sigma_g^+)$, (23) O_2^+, (24) O_4^+, (25) OH^+, (26) H_2O^+, (27) OH^-, (28) H_3O^+, (29) $O_3H_2^+$.

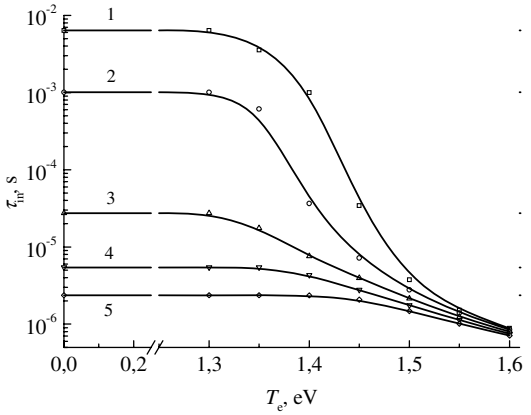

Fig. 27 Ignition time of H_2-O_2 stoichiometric (67–33%) mixture vs electron temperature at $p = 1$ atm and at instant gas heating to various initial gas temperatures T_0, K: (1) 800, (2) 900, (3) 1000, (4) 1100, (5) 1200.

induction period. Recombination and recharged collisions of ions, processes of attachment and detachment, result in an establishment of balance of concentration of the charged particles. Thus, at a stage previous to ignition of a hydrogen–oxygen mixture, the H_5^+ ion is the basic positive ion in the discharge, and the ion O_3^- is the basic negative ion.

Gas-discharge influence on the induction period of H_2-O_2 stoichiometric (67–33%) mixture is shown in Fig. 27 at $p = 1$ atm and at instant gas heating to various initial gas temperatures T_0. Figure 27 shows that time of an ignition delay under condition of the gas discharge (that is at high value of reduced electric field) is decreased to some orders of values at low gas temperature. Calculations have also shown that, at increase in the percentage of hydrogen in the H_2-O_2 mixture, the gas discharge results in the greater decreasing of ignition delay time in comparison with stoichiometric mixture, whereas the influence of the gas discharge on ignition of poor mixtures is less significant.

For determination of the basic channels influencing ignition time delay under conditions of gas discharge, the reduction of the used initial kinetic scheme has been carried out [25]. Three reduced kinetic schemes have been considered. The first scheme consists of 27 components and 104 reactions, the second one contains 21 components and 89 reactions, and the third scheme includes 21 components and 82 reactions. Our studies have shown that the reduced kinetic scheme containing 21 components and 89 reactions is sufficient to accuracy describe the process of ignition of H_2-O_2 mixture at various values of the mixture composition, total densities, gas temperatures, and electronic temperatures. In a wide range of conditions, the induction time calculated with this kinetic scheme differs from the induction time calculated with the initial (full) kinetic scheme by no more than 10%. However, if experimental conditions are not known beforehand, it is necessary to apply the initial not-reduced kinetic scheme to the modeling of ignition. To reveal the contribution of different components, and also the main channels rendering the basic influence on acceleration or deceleration of chain reaction of ignition of the hydrogen–oxygen mixture, the investigations of sensitivity of the kinetic model in relation to time of an induction have been carried out with the help of the second reduced kinetic scheme at various conditions [25].

VI. Conclusions

A new technique for exciting a discharge in a gas flow is considered. The properties of freely localized and surface microwave discharges in air and in supersonic air–propane flows have been investigated experimentally. Initiating microwave discharges are a reliable and efficient way of generating a low-temperature plasma in a supersonic airflow and of initiating the combustion of supersonic flows of hydrocarbon fuels. Received results testify to the efficiency of the use of the combined microwave discharge in plasma aerodynamics.

Acknowledgments

This work was partially supported by the Russian Foundation of Basic Research (grant nos. 02-02-17116, 05-02-16532, and 08-02-01251) and the European Office of Aerospace Research and Development (International Science and Technology Center grant no. 2248p).

References

[1] *International Space Planes and Hypersonic System and Technologies Conference. Workshop on Weakly Ionized Gases*, AIAA, Reston, VA, 1997–2006.

[2] "International Workshops on Magneto- and Plasma Aerodynamics for Aerospace Applications," *Proceedings, Inst. of High Temperatures of the Russian Academy of Sciences*, Moscow, 1999–2003, 2005.

[3] Semenov, N. N., *Tsepnye Reaktsii* (Chain Reactions), Nauka, Moscow, 1986 [in Russian].

[4] Lewis, B., and Von Elbe, G., *Combustion, Flames and Explosions of Gases*, Academic, New York, 1961.

[5] Coffee, T. R., "Kinetic Mechanisms for Premixed, Laminar, Steady State Methane/Air Flames," *Combustion and Flame*, Vol. 55, No. 2, 1984, pp. 161–170. doi:10.1016/0010-2180(84)90024-5

[6] Frenklach, M., and Bornside, D. E., "Shock-Initiated Ignition in Methane-Propane Mixtures," *Combustion and Flame*, Vol. 56, No. 1, 1984, pp. 1–27. doi:10.1016/0010-2180(84)90002-6

[7] Seery, D. J., and Bowman, C. T., "An Experimental and Analytical Study of Methane Oxidation Behind Shock Waves," *Combustion and Flame*, Vol. 14, No. 1, 1970, pp. 37–48. doi:10.1016/S0010-2180(70)80008-6

[8] Azatyan, V. V., "New Laws in Gas Phase Branched–Chain Processes," Ph.D. Dissertation, Inst. of Chemical Physics, Moscow, 1978 [in Russian].

[9] Dautov, N. G., and Starik, A. M., "On the Problem of Choosing a Kinetic Scheme for Description of the Volume Reaction of Methane with Air," *Kinetika i Kataliz*, Vol. 38, No. 2, 1997, pp. 207–230 [in Russian].

[10] Starik, A. M., Titova, N. S., and Yanovskiy, L. S., "Peculiarity of Kinetics of Oxidation of Destruction Products of C_3H_8 and C_4H_{10} with Air Mixture," *Kinetika i Kataliz*, Vol. 40, No. 1, 1999, pp. 11–26 [in Russian].

[11] Semenov, N. N., "*O Nekotorykh Problemakh Khimicheskoy Kinetiki i Reaktsionnoi Sposobnosti (Some Problems of Chemical Kinetics and Reactivity)*," Akademiya Nauk, Moscow, 1958 [in Russian].

[12] Nalbandyan, A. B., and Voevodskii, V. V., "Mechanism of Oxidation and Burning of Hydrogen," Akademiya Nauk, Moscow, 1949 [in Russian].

[13] Bozhenkov, S. A., Starikovskaya, S. M., and Starikovskii, A. Y., "Nanosecond Gas Discharge Ignition of H_2- and CH_4-Containing Mixtures," *Combustion and Flame*, Vol. 133, Nos. 1–2, 2003, pp. 133–146. doi:10.1016/S0010-2180(02)00564-3

[14] Seleznev, A. A., Aleinikov, A. Yu., and Yaroshenko, V. V., "Influence of Radiolysis on Displacement of Limits of Ignition of a Hydrogen–Oxygen Gas Mixture," *Khimicheskaia Fizika*, Vol. 18, No. 5, 1999, pp. 65–71 [in Russian].

[15] Tanoff, M. A., Smooke, M. D., Teets, K. E., and Sell, J. A., "Computational and Experimental Studies of Laser-Induced Thermal Ignition in Premixed Ethylene-Oxidizer Mixtures," *Combustion and Flame*, Vol. 103, No. 4, 1995, pp. 253–280. doi:10.1016/0010-2180(95)00098-4

[16] Ma, J. X., Alexander, D. R., and Poulain, D. E., "Laser Spark Ignition and Combustion Characteristics of Methane-Air Mixtures," *Combustion and Flame*, Vol. 112, No. 4, 1998, pp. 492–506. doi:10.1016/S0010-2180(97)00138-7

[17] Morsy, M. H., Ko, Y. S., and Chung, S. H., "Laser-Induced Ignition a Conical Cavity IN CH_4-Air Mixtures," *Combustion and Flame*, Vol. 119, No. 4, 1999, pp. 473–482. doi:10.1016/S0010-2180(99)00060-7

[18] Esakov, I. I., Grachev, L. P., Khodataev, K. V., Vinogradov, V. A., and Van Wie, D., "Propane-Air Mixture Combustion Efficiency in Deeply Undercritical MW Discharge Area in Cold High-Speed Airflow," AIAA Paper 2006-1212, 2006.

[19] Shibkov, V. M., Alexandrov, A. F., Chernikov, A. V., Ershov, A. P., Shibkova, L. V., and Timofeev, I. B., "Freely Localized Microwave Discharge in a Supersonic Flow," AIAA Paper 2001-2946, 2001.

[20] Shibkov, V. M., Abramova, A. D., Chernikov, V. A., Ershov, A. P., Gromov, V. G., Karachev, A. A., Konstantinovskij, R. S., Shibkova, L. V., Timofeev, I. B., and Voskanyan, A. V., "Microwave Discharges in Supersonic Plasma Aerodynamics," AIAA Paper 2004–0513, 2004.

[21] Shibkov, V. M., Chernikov, V. A., Ershov, A. P., Konstantinovskij, R. S., Shibkova, L. V., and Zlobin, V. V., "Propane-Butane-Air Mixture Ignition and Combustion in the Aerodynamic Channel with the Stagnant Zone," AIAA Paper 2004-0838, 2004.

[22] Shibkov, V. M., and Konstantinovskii, R. S., "Kinetic Model of Ignition of Hydrogen-Oxygen Mixture Under Conditions of Non-Equilibrium Plasma of the Gas Discharge," AIAA Paper 2005-0987, 2005.

[23] Shibkov, V. M., Chernikov, A. V., Georgievskiy, P. Yu., Gromov, V. G., Ershov, A. P., Karachev, A. A., Konstantinovskij, R. S., and Levin, V. A., "Influence of Surface Microwave Discharge on the Characteristics of Supersonic Flow Near to a Streamlined Body," AIAA Paper 2005-0779, 2005.

[24] Shibkov, V. M., Aleksandrov, A. F., Chernikov, V. A., Dvinin, S. A., Ershov, A. P., Shibkova, L. V., Abramova, A. D., Konstantinovskij, R. S., Surkont, O. S., Voskanyan, A. V., and Zlobin, V. V., "Surface Microwave Discharge in Air," AIAA Paper 2006-1216, 2006.

[25] Konstantinovskii, R. S., Shibkov, V. M., and Shibkova, L. V., "Effect of a Gas Discharge on the Ignition in the Hydrogen–Oxygen System," *Kinetics and Catalysis*, Vol. 46, No. 6, 2005, pp. 775–778. [Translated from *Kinetika i Kataliz*, Vol. 46, No. 6, 2005, pp. 821–834.] doi:10.1007/s10975-005-0136-2

[26] Shibkov, V. M., Aleksandrov, A. F., Ershov, A. P., Timofeev, I. B., Chernikov, V. A., and Shibkova, L. V., "Freely Localized Microwave Discharge in a Supersonic Gas Flow," *Plasma Physics Reports*, Vol. 31, No. 9, 2005, pp. 795–801. [Translated from *Fizika Plasmy*, Vol. 31, No. 9, pp. 857–864.] doi:10.1134/1.2048839

[27] Shibkov, V. M., Alexandrov, A. F., Ershov, A. P., Karachev, A. A., Konstantinovskij, R. S., Timofeev, I. B., Chernikov, V. A., and Shibkova, L. V., "Ignition of Supersonic Stream of Hydrocarbon Fuel with the Help of Microwave Discharges," *Moscow University Physics Bulletin*, Vol. 59, No. 5, 2004, pp. 64–66. [Translated from *Vestnik Moskovskogo Univ.*, Series 3, Fizika. Astronomiya, No. 5, 2004, pp. 67–69.]

[28] Zlobin, V. V., Kuzovnikov, A. A., and Shibkov, V. M., "Concentration of Electrons in a Stimulated Microwave Discharge Channel in Nitrogen," *Moscow University Physics Bulletin*, Vol. 43, No. 1, 1988, pp. 98–100. [Translated from *Vestnik Moskovskogo Univ.*, Series 3, Fizika. Astronomiya, Vol. 29, No. 1, 1988, pp. 89–91.]

[29] Devyatov, A. M., Kuzovnikov, A. A., Lodinev, V. V., and Shibkov, V. M., "The Mechanism of Molecular Gas Heating in a Pulsed Free-Localizing RF Discharge," *Moscow University Physics Bulletin*, Vol. 46, No. 2, 1991, pp. 28–31. [Translated from *Vestnik Moskovskogo Univ.*, Series 3, Fizika. Astronomiya, Vol. 32, No. 2, 1991, pp. 29–33.]

[30] Alexandrov, A. F., Kuzovnikov, A. A., and Shibkov, V. M., "Freely Localized Microwave Discharge in a Focused Beam," *Inzhenerno-Fizicheskiy Zhurnal*, Vol. 62, No. 5, 1992, pp. 726–732 [in Russian].

[31] Alexandrov, A. F., Kuzovnikov, A. A., Shibkov, V. M., Shibkova, L. V., and Zlobin, V. V., "Parameters, Kinetics, Experimental and Mathematical Modeling Non-Equilibrium Plasma of a Freely Localized Microwave Discharge in Air," *Applied Physics*, Vol. 4, No. 4, 1994, pp. 20–29 [in Russian].

[32] Zarin, A. S., Kuzovnikov, A. A., and Shibkov, V. M., "*Svobodno Lokalizovannyi SVCh Razryad v Vozdukhe (Freely Localized Microwave Discharge in Air)*," Neft' i Gaz, Moscow, 1996 [in Russian].

[33] Kuzovnikov, A. A., Shibkov, V. M., and Shibkova, L. V., "Free-Localized Pulse-Periodic MW Discharge in Air. Kinetics of Gas Heating," *High Temperature*, Vol. 34, No. 3, 1996, pp. 343–348. [Translated from *Teplofizika Vysokikh Temperatur*, Vol. 34, No. 3, 1996, pp. 349–354.]

[34] Shibkov, V. M., "Free-Localized Pulse-Periodic MW Discharge in Air. Electric Field Strength in Plasma," *High Temperature*, Vol. 34, No. 4, 1996, pp. 519–524. [Translated from *Teplofizika Vysokikh Temperatur*, Vol. 34, No. 4, 1996, pp. 525–530.]

[35] Kuzovnikov, A. A., Shibkov, V. M., and Shibkova, L. V., "Kinetics of Charged Particles in a Free-Localized Pulse-Periodic MW Discharge in Air," *High Temperature*, Vol. 34, No. 5, 1996, pp. 651–655. [Translated from *Teplofizika Vysokikh Temperatur*, Vol. 34, No. 5, 1996, pp. 741–745.]

[36] Kalinin, A. V., Shibkov, V. M., and Shibkova, L. V., "Influence of Oxygen on Kinetics of Heating of Molecular Gas in a N_2-O_2 Mixture," *Moscow University Physics Bulletin*, Vol. 51, No. 1, 1996, pp. 38–42. [Translated from *Vestnik Moskovskogo Univ.*, Series 3, Fizika. Astronomiya, Vol. 37, No. 1, 1996, pp. 38–42.]

[37] Lodinev, V. V., Shibkov, V. M., and Shibkova, L. V., "Gas Heating Kinetics in Pulse-Periodic Air Discharge," *Moscow University Physics Bulletin*, Vol. 51, No. 2, 1996, pp. 26–31. [Translated from *Vestnik Moskovskogo Univ.*, Series 3, Fizika. Astronomiya, Vol. 37, No. 2, 1996, pp. 29–35.]

[38] Shibkov, V. M., "Heating of Gas Under Conditions of Free-Localized Microwave Discharge in Air. Mathematical Simulation," *High Temperature*, Vol. 35, No. 5, 1997, pp. 681–689. [Translated from *Teplofizika Vysokikh Temperatur*, Vol. 35, No. 5, 1997, pp. 693–701.]

[39] Shibkov, V. M., "Heating of Gas Under Conditions of Free-Localized Microwave Discharge in Air: Experiment," *High Temperature*, Vol. 35, No. 6, 1997, pp. 858–862. [Translated from *Teplofizika Vysokikh Temperatur*, Vol. 35, No. 6, 1997, pp. 693–701.]

[40] Kuzovnikov, A. A., Shibkov, V. M., and Shibkova, L. V., "Kinetics of Electrons in Plasma of Discharge, Created in Free Space by Focused Microwave Beam," *Technical Physics*, Vol. 67, No. 6, 1997, pp. 10–18. [Translated from *Zhurnal Tekhnicheskoy Fiziki*, Vol. 67, No. 6, 1997, pp. 10–14.]

[41] Alexandrov, A. F., Zarin, A. S., Kuzovnikov, A. A., Shibkov, V. M., and Shibkova, L. V., "Plasma Parameters of Non-Consistent Microwave Discharge, Created in Programmable Pulse," *Technical Physics*, Vol. 67, No. 7, 1997, pp. 19–23. [Translated from *Zhurnal Tekhnicheskoy Fiziki*, Vol. 67, No. 7, 1997, pp. 19–23.]

[42] Zlobina, Yu. V., Shibkov, V. M., and Shibkova, L. V., "Kinetics of Heating and Dissociation of Molecules in Pulsed Discharge in Hydrogen," *Plasma Physics Reports*, Vol. 24, No. 7, 1998, pp. 617–621. [Translated from *Fizika Plasmy*, Vol. 24, No. 67, 1998, pp. 667–671.]

[43] Shibkov, V. M., Vinogradov, D. A., Voskanyan, A. V., Ershov, A. P., Timofeev, I. B., Shibkova, L. V., and Chernikov, V. A., "Surface Microwave Discharge in Supersonic Airflow," *Moscow University Physics Bulletin*, Vol. 55, No. 6, 2000, pp. 80–82. [Translated from *Vestnik Moskovskogo Univ.*, Series 3, Fizika. Astronomiya, Vol. 41, No. 6, 2000, pp. 64–66.]

[44] Shibkov, V. M., Chernikov, A. V., Chernikov, V. A., Ershov, A. P., Shibkova, L. V., Timofeev, I. B., Vinogradov, D. A., and Voskanyan, A. V., "Surface Microwave Discharge on Dielectric Body in a Supersonic Flow of Air," *Microwave Discharges: Fundamentals and Applications*, Yanus-K, Moscow, 2001, pp. 145–153.

[45] Shibkov, V. M., Chernikov, V. A., Dvinin, S. A., Ershov, A. P., Shibkova, L. V., Timofeev, I. B., Vinogradov, D. A., and Voskanyan, A. V., "Dense Large-Diameter Uniform Plasma of a Surface Microwave Discharge," *Proceedings of the 15th International Symposium on Plasma Chemistry*, Vol. 1, Orleans, France, 2001, pp. 179–184.

[46] Shibkov, V. M., Ershov, A. P., Chernikov, V. A., and Shibkova, L. V., "Microwave Discharge on the Surface of a Dielectric Antenna," *Technical Physics*, Vol. 50, No. 4, 2005, pp. 455–461. [Translated from *Zhurnal Tekhnicheskoy Fiziki*, Vol. 75, No. 4, 2005, pp. 67–73.] doi:10.1134/1.1901784

[47] Shibkov, V. M., Dvinin, S. A., Ershov, A. P., and Shibkova, L. V., "Mechanisms of Microwave Surface Discharge Propagation," *Technical Physics*, Vol. 50, No. 4, 2005, pp. 462–467. [Translated from *Zhurnal Tekhnicheskoy Fiziki*, Vol. 75, No. 4, 2005, pp. 74–79.] doi:10.1134/1.1901785

[48] Litvak, A. G. (ed.), "*High-Frequency Discharge in Wave Fields*," Inst. Prikladnoy Fiziki, Akademiya Nauk (Inst. of Applied Physics of the Academy of Sciences of the USSR), Gorky, Russia, 1988 [in Russian].

[49] Litvak, A. G. (ed.), "*International Workshops on Strong Microwaves in Plasmas*," Vols. 1–2, Nizhny Novgorod, Russia, 1991, 1994, 2003.

[50] Batanov, G. M., Gritsinin, S. I., and Kossy, I. A., "High Pressure Microwave Discharges," *Trudy Fizicheskogo Instituta im. P.N.Lebedeva*, Vol. 160, Academy of Sciences of USSR, Moscow, 1985, pp. 174–203 [in Russian].

[51] Gil'denburg, V. V., and Golubev, S. V., "Nonequilibrium High-Frequency Discharge in Wave Fields," *Zhurnal Eksperimentalnoy i Teoretichaskoy Fiziki (Journal of Experimental and Theoretical Physics)*, Vol. 67, No. 1(7), 1974, pp. 89–93 [in Russian].

[52] Vikharev, A. L., Gil'denburg, V. B., and Golubev, S. V., "Nonlinear Dynamics of Freely Localized Microwave Discharge in a Beam of Electromagnetic Waves," *Zhurnal Eksperimentalnoy i Teoretichaskoy Fiziki (Journal of Experimental and Theoretical Physics)*, Vol. 94, No. 4, 1988, pp. 135–145 [in Russian].

[53] Batskikh, G. I., and Khvorostyanoi, Yu. I., "Experimental Installation for Creation of Power Focused Microwave Flow in a Free Space," *Radiotekhnika i Elektronika*, Vol. 37, No. 2, 1992, pp. 311–315 [in Russian].

[54] Brovkin, V. G., and Kolesnichenko, Yu. F., "Classification of

Microwave Discharge Structures," *Pis'ma v Zhurnal Teknicheskoy Fiziki (Soviet Technical Physics Letters)*, Vol. 16, No. 3, 1990, pp. 55–58 [in Russian].

[55] Khodataev, K. V., "Various Types of Initiators for Attached Undercritical MW Discharge Ignition," AIAA Paper 2007-0431, 2007.

[56] Moisan, M., Zakrzhewski, Z., and Pantel, R., "Theory and Characteristics of an Efficient Surface Wave Launcher (Surfatron) Producing Long Plasma Column," *Journal of Physics D: Applied Physics*, Vol. 12, No. 2, 1979, pp. 219–237. doi:10.1088/0022-3727/12/2/008

[57] Daviaud, S., Boisse-Laporte, C., Leprince, P., and Marec, J., "Description of Surface-Wave-Produced Microwave Discharge in Helium at Low Pressure in the Presence of a Gas Flow," *Journal of Physics D: Applied Physics*, Vol. 22, No. 6, 1989, pp. 770–779. doi:10.1088/0022-3727/22/6/009

[58] Granier, A., Boisse-Laporte, C., Leprince, P., Marec, J., and Nghiem, P., "Wave propagation and diagnostics in argon surface-wave discharges up to 100 Torr," *Journal of Physics D: Applied Physics*, Vol. 20, No. 2, 1987, pp. 204–209. doi:10.1088/0022-3727/20/2/009

[59] Marec, J., and Leprince, P., "Recent Trends and Developments of Microwave Discharges," *Journal de Physique IV, Proceedings*, Vol. 8, No. PR7, 1998, pp. 21–32.

[60] Zakrzhewski, Z., "Condition of Existence and Axial Structure of Long Microwave Structure, Sustained by Traveling Microwave," *Journal of Physics D: Applied Physics*, Vol. 16, No. 2, 1983, pp. 171–181. doi:10.1088/0022-3727/16/2/014

[61] Dvinin, S. A., Dovzhenko, V. A., and Solntzev, G. S., "On the Change of Power Characteristics of the Microwave Discharge at Development of Ionized Instability on a Surface Wave," *Fizika Plasmy*, Vol. 9, No. 5, 1983, pp. 1058–1067 [in Russian].

[62] Matveev, A. A., and Silakov, V. P., "Non-Equilibrium Kinetic Processes in Low-Temperature Hydrogen Plasma," Preprint No. 8, General Physics Inst. of the Russian Academy of Sciences, Moscow, 1994, pp. 1–30 [in Russian].

[63] Raizer, Yu. P., *Gas Discharge Physics*, Springer–Verlag, Berlin, 1991.

[64] Mayhan, J. T., Fante, R. L., O'Keefe, R., Elkin, R., Klugerman, J., and Yos, J., "Comparison of Various Microwave Breakdown Prediction Models," *Journal of Applied Physics*, Vol. 42, No. 13, 1971, pp. 5362–5369. doi:10.1063/1.1659950

[65] Babaeva, N. Yu., Mnatsakanyan, A. X., and Naidis, G. V., "Dynamics of Discharges in Nitrogen in Beams of Electromagnetic Waves," *Plasma Physics Reports*, Vol. 18, No. 8, 1992, pp. 1055–1063.

S. Macheret
Associate Editor